Universality of modulation length and time exponents

Saurish Chakrabarty,[1] Vladimir Dobrosavljević,[2] Alexander Seidel,[1] and Zohar Nussinov[1,3,*]
[1]*Department of Physics and Center for Materials Innovation, Washington University in St. Louis, Missouri 63130, USA*
[2]*Department of Physics and National High Magnetic Field Laboratory, Florida State University, Tallahassee, Florida 32306, USA*
[3]*Kavli Institute for Theoretical Physics, Santa Barbara, California 93106, USA*
(Received 27 April 2012; published 18 October 2012)

We study systems with a crossover parameter λ, such as the temperature T, which has a threshold value λ_* across which the correlation function changes from exhibiting fixed wavelength (or time period) modulations to continuously varying modulation lengths (or times). We introduce a hitherto unknown exponent ν_L characterizing the universal nature of this crossover and compute its value in general instances. This exponent, similar to standard correlation length exponents, is obtained from motion of the poles of the momentum (or frequency) space correlation functions in the complex k-plane (or ω-plane) as the parameter λ is varied. Near the crossover (i.e., for $\lambda \to \lambda_*$), the characteristic modulation wave vector K_R in the variable modulation length "phase" is related to that in the fixed modulation length "phase" q via $|K_R - q| \propto |T - T_*|^{\nu_L}$. We find, in general, that $\nu_L = 1/2$. In some special instances, ν_L may attain other rational values. We extend this result to general problems in which the eigenvalue of an operator or a pole characterizing general response functions may attain a constant real (or imaginary) part beyond a particular threshold value λ_*. We discuss extensions of this result to multiple other arenas. These include the axial next-nearest-neighbor Ising (ANNNI) model. By extending our considerations, we comment on relations pertaining not only to the modulation lengths (or times), but also to the standard correlation lengths (or times). We introduce the notion of a Josephson time scale. We comment on the presence of aperiodic "chaotic" modulations in "soft-spin" and other systems. These relate to glass-type features. We discuss applications to Fermi systems, with particular application to metal to band insulator transitions, change of Fermi surface topology, divergent effective masses, Dirac systems, and topological insulators. Both regular periodic and glassy (and spatially chaotic behavior) may be found in strongly correlated electronic systems.

DOI: 10.1103/PhysRevE.86.041132 PACS number(s): 05.50.+q, 75.10.Hk, 75.60.Ch

I. INTRODUCTION

In complex systems, there are, in general, possibly many important length and time scales that characterize correlations. Aside from correlation lengths describing the exponential decay of correlations, in some materials there are length scales that characterize periodic spatial modulations or other spatially nonuniform properties as in Fig. 1. We investigate the evolution of these length scales as a function of some parameter λ. This parameter may be the temperature, the chemical potential, or some other physical quantity relevant for description of the system being studied. To illustrate our basic premise, we will largely focus on temperature dependencies of the correlation function in this work. However, with a trivial change of variables, our results are valid for any parameter that, when tuned, connects a phase with continuously varying modulation lengths (or times) to one in which the modulation length (or time) is pinned to a fixed value. The crossovers we consider are not symmetry breaking transitions. Consequences of our considerations also relate to correlation lengths as we will comment on later.

Many systems exhibit subtle changes in their correlation functions at certain special temperatures. The main focus of our work pertains to the following situation. As the temperature is varied across a certain crossover temperature T_*, an unmodulated phase of a system may start exhibiting modulations, even though a thermodynamic phase transition does not occur. A generalization of this occurs when modulations in a system are characterized by a fixed wavelength on one side of a crossover temperature and by continuously varying wavelengths on the other side. Such an occurrence may generally be seen when interactions of different scales compete with one another. A wealth of interesting periodic spatial patterns appear in disparate arenas: e.g., the manganites [2], pnictide [3,4], and cuprate [5–10] superconductors, quantum Hall systems [11–13], dense nuclear matter [14,15], magnetic systems [16–21], heavy fermion compounds [22,23], membranes [24] cholesterols [25], magnetic garnets [26], dipolar systems [27,28], systems with nematic phases [29], and countless other systems [30–34].

II. OUR MAIN RESULTS AND THEIR IMPLICATIONS

In this work, we report on the temperature (or other parameter) dependence of emergent modulation lengths that govern the size of various domains present in some systems. In its simplest incarnation, our central result is that if fixed wavelength modulations characterized by a particular *finite* length scale L_* appear beyond some temperature T_*, then, the modulation length L_D on the other side of the crossover differs from L_* as

$$|L_D - L_*| \propto |T - T_*|^{\nu_L}. \tag{1}$$

When there are *no modulations* on one side of T_*, i.e., $L_* \to \infty$, we have near the crossover

$$L_D \propto |T - T_*|^{-\nu_L}. \tag{2}$$

Apart from some special situations, we find that irrespective of the interaction, $\nu_L = 1/2$. We arrive at this rather universal

*zohar@wuphys.wustl.edu

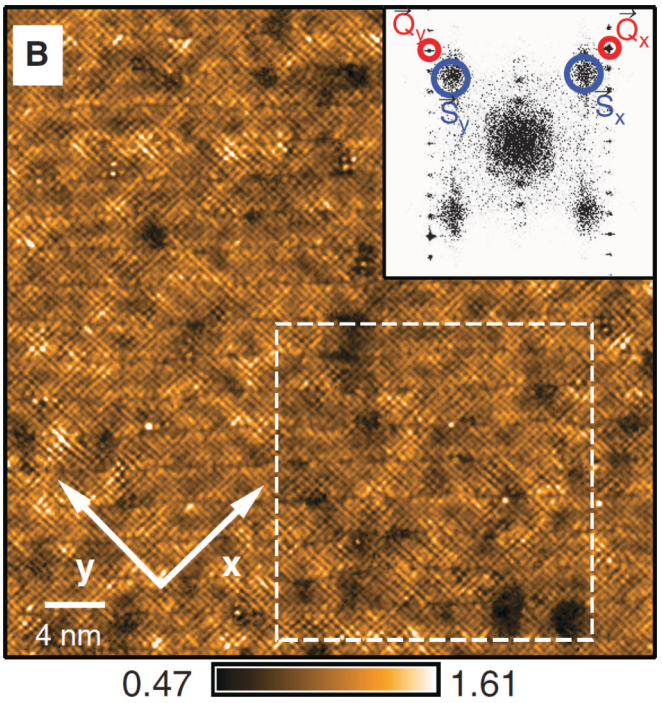

FIG. 1. (Color online) Sub-unit-cell resolution image of the electronic structure of a cuprate superconductor at the pseudogap energy. Inset shows Fourier space image of the same figure. Nematic and smectic phases are highlighted using the red (small) and blue (large) circles, respectively. The nematic phase is characterized by commensurate wave vectors $\vec{Q}$. The smectic wave vector, on the other hand, takes incommensurate value $\vec{S}$, which is dependent on the amount of doping, albeit weakly. (From Ref. [1]; reprinted with permission from AAAS.)

result assuming that there is no phase transition at the crossover temperature T_*. Our result holds everywhere inside a given thermodynamic phase of a system.

The large n Coulomb frustrated ferromagnet. The reader might find it useful to think about the Coulomb frustrated ferromagnet in the back of his/her mind when thinking about the above result. This was discussed in Ref. [35] and will be further elaborated in Sec. V C. In this system, the modulation length diverges across a crossover temperature T_* exhibiting an exponent of $\nu_L = 1/2$.

Our considerations are not limited to continuous crossovers. A corollary of our analysis pertains to systems with discontinuous (*"first-order"-like*) jumps in the correlation or modulation lengths.

We will further comment on situations wherein a branch point appears at T_*. We will present examples where we obtain rational and irrational exponents and also the anomalous critical exponent η. Our analysis affords general connections to the critical scaling of correlation lengths in critical phenomena.

Our results for spatial dependence of the correlation functions can be extended to the time domain. Amongst other notions, by a formal interchange of spatial with temporal coordinates, we introduce the concept of a *Josephson time scale*. Similarly, by further deepening the analogy between results in the spatial and temporal domains, we will comment on the presence of phases with aperiodic or "chaotic" spatial modulations (characteristic of amorphous configurations) in systems governed by nonlinear Euler-Lagrange equations. Such aperiodic or "chaotic" modulations may appear in strongly correlated electronic systems.

In Appendix A, we present applications to Fermi systems pertaining to metal-band insulator transition, change of Fermi surface topology, divergence of effective masses, Dirac systems, and topological insulators.

III. SYSTEMS OF STUDY

In this work, we will predominantly consider translationally invariant systems on a lattice, the Hamiltonian of which is given by

$$H = \frac{1}{2}\sum_{\vec{x}\neq\vec{y}} V(|\vec{x}-\vec{y}|)S(\vec{x})S(\vec{y}). \tag{3}$$

The quantities $\{S(\vec{x})\}$ portray classical scalar spins or fields. The sites $\vec{x}$ and $\vec{y}$ lie on a d-dimensional hypercubic (or some other) lattice with N sites. We will set the lattice constant to unity. [In the quantum arena, we replace the spins $\vec{S}(\vec{x})$ in Eq. (3) by Fermi or Bose or quantum spin operators.]

The results that will be derived in this work apply to a variety of systems. These include theories with trivial n-component generalizations of Eq. (3). In the bulk of this work, the Hamiltonian has a bilinear form in the spins. We will, however, later on, study "soft"-spin model with explicit finite quartic terms as we now expand on. An n-component generalization of Eq. (3) is given by the Hamiltonian

$$H = \frac{1}{2}\sum_{\vec{x}\neq\vec{y}} V(|\vec{x}-\vec{y}|)\vec{S}(\vec{x})\cdot\vec{S}(\vec{y}) + \frac{u}{4}\sum_{\vec{x}}(\vec{S}(\vec{x})\cdot\vec{S}(\vec{x})-n)^2. \tag{4}$$

Such a Hamiltonian represents standard (or "hard") spin or $O(n)$ systems in the large u limit ($u \gg 1$). The quartic term enforces a "hard" normalization constraint of the particular form $\vec{S}(\vec{x})\cdot\vec{S}(\vec{x}) = n$. For finite (or small) u, Eq. (4) describes "soft"-spin systems wherein the normalization constraint is not strictly enforced.

In what follows, $v(\vec{k})$ and $s(\vec{k})$ will denote the Fourier transforms of $V(|\vec{x}-\vec{y}|)$ and $S(\vec{x})$. We employ the following Fourier conventions:

$$a(\vec{k}) = \sum_{\vec{x}} A(\vec{x})e^{i\vec{k}\cdot\vec{x}}, \quad A(\vec{x}) = \frac{1}{N}\sum_{\vec{k}} a(\vec{k})e^{-i\vec{k}\cdot\vec{x}}. \tag{5}$$

With these conventions in tow, in Fourier space, Eq. (3) reads as

$$H = \frac{1}{2N}\sum_{\vec{k}} v(\vec{k})|s(\vec{k})|^2. \tag{6}$$

When $v(\vec{k})$ is analytic in all momentum space coordinates, it is a function of $|\vec{k}|^2 = k^2$ (and not a general function of $k \equiv \sqrt{\sum_{l=1}^{d} k_l^2}$ with $\{k_l\}$ being the Cartesian components of $\vec{k}$). This is so as $|\vec{k}|$ has branch cuts when viewed as a function of a particular k_l (with all other $k_{l'\neq l}$ held fixed). The lattice Laplacian that links nearest-neighbor sites in real

space becomes

$$\Delta_{\vec{k}} = 2\sum_{l=1}^{d}(1-\cos k_l) \tag{7}$$

in k space. $\Delta_{\vec{k}}$ veers towards $|\vec{k}|^2$ in the continuum (small k) limit. The two point correlation function for the system in Eq. (3) is $G(\vec{x}) = \langle S(0)S(\vec{x})\rangle$. At large distances, $x = |\vec{x}|$, the correlation function has a general asymptotic behavior

$$G(x) \approx \sum_i f_i(x)\cos\left(\frac{2\pi x}{L_D^{(i)}}\right)e^{-x/\xi_i}. \tag{8}$$

In the ith term, $f_i(x)$ is an algebraic prefactor, $L_D^{(i)}$ is the modulation length, and ξ_i is the corresponding correlation length. In general, the function $f_i(x)$ may contain a factor with an anomalous exponent η (usually not an integer), such as $f_i(x) \propto 1/x^{d-2+\eta}$. Generally, there can be multiple correlation and modulation lengths. In Fourier space, $G(\vec{k}) = \frac{1}{N}\langle|s(\vec{k})|^2\rangle$. The modulation and correlation lengths can be obtained, respectively, from the real and imaginary parts of the poles of $G(\vec{k})$ in the complex k plane.

A. General considerations: Correlation and modulation lengths from momentum space correlation function

The correlation function $G(\vec{x})$ in (d-dimensional) real space is related to the momentum space correlation function $G(\vec{k})$ by

$$G(\vec{x}) = \int \frac{d^dk}{(2\pi)^d}G(\vec{k})e^{-i\vec{k}\cdot\vec{x}}. \tag{9}$$

On the lattice, the integral above must be replaced by summation over $\vec{k}$ values belonging to the first Brillouin zone. In the continuum, which we discuss here, the integral range is unbounded. Even in lattice systems, doing an unbounded summation over $\vec{k}$ values provides a good approximation for the correlation function in real space in many scenarios.

For spherically symmetric problems, i.e., when $G(\vec{k}) = G(k)$,

$$G(x) = \int_0^\infty \frac{k^{d-1}dk}{(2\pi)^{d/2}}\frac{\mathrm{J}_{d/2-1}(kx)}{(kx)^{d/2-1}}G(k), \tag{10}$$

where $\mathrm{J}_\nu(x)$ is a Bessel function of order ν. The above integral can be evaluated by choosing an appropriate contour in the complex k plane. The contour can be closed along a circular arc of radius $R \to \infty$ provided

$$|G(k)| \lesssim k^{-\frac{d+1}{2}} \text{ as } k \to \infty. \tag{11}$$

In evaluating the integral in Eq. (10), we obtain contributions from residues associated with the poles of the integrand as well as contributions from its branch points. We use $K = K_R + iK_I$ to represent the poles and branch points of the integrand in the complex plane. The correlation and modulation lengths in the system are determined, respectively, by the imaginary (K_I) and real parts (K_R) of these poles and branch points. Together, all these singularities can be compactly expressed as

$$\boxed{\frac{1}{G^{(m)}(K)} = 0}, \tag{12}$$

where $0 \leqslant m < \infty$ is the order of the smallest order derivative of $G(k)$ which diverges at $k = K$ [36].

In Ref. [37], we comment on the situation in which the function $G(T,k)$ is an entire function of k (i.e., when G is analytic everywhere).

IV. A UNIVERSAL DOMAIN LENGTH EXPONENT: DETAILS OF ANALYSIS

We now derive (via various interrelated approaches) our central result: the existence of a domain length exponent in rather general systems with real or complex scalar fields, vectorial (or tensorial) fields of both the discrete (e.g., Potts type) and continuous variants.

We will now consider the situation in which the system exhibits modulations at a fixed wave vector q for a finite range of temperatures on one side of T_* [viz., (i) $T > T_*$ or (ii) $T < T_*$] and starts to exhibit variable wavelength modulations on the other side [(iii) $T < T_*$ for (i) and $T > T_*$ for (ii)]. A schematic illustrating this is shown in Fig. 2. In Sec. IV A, we will assume that the pair correlation function is meromorphic (realized physically by *absence of phase transitions*) at the crossover point and illustrate how modulation length exponents may appear. In Sec. IV D, we will comment on the situation where the crossover point may be a branch point of the correlation function.

A. Crossovers at general points in the complex k plane

In the up and coming, we will assume that the pair correlator $G(T,k)$ is a meromorphic function of k and T near a crossover point. Our analysis below is exact as long as we do not

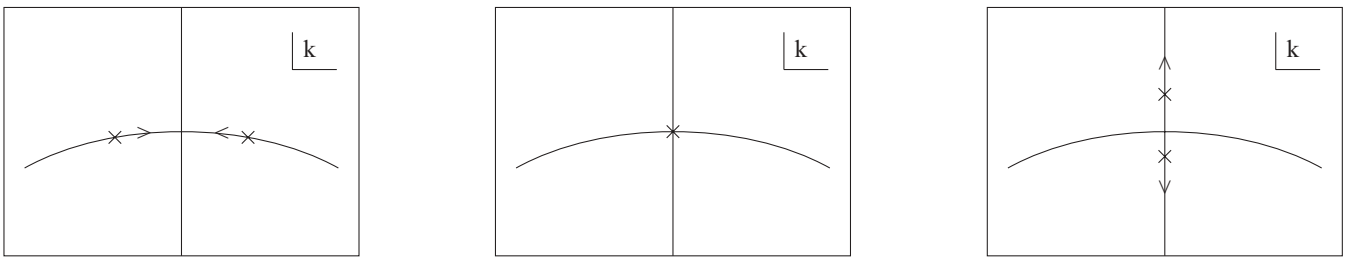

(a)Variable modulation length. (b)The crossover point ($T = T_*$). (c)Fixed modulation length.

FIG. 2. Schematic showing the trajectories of the singularities of the correlation function near a fixed-variable modulation length crossover. Two poles of the correlation function merge at $k = k_*$ at $T = T_*$. On the fixed modulation length side of the crossover point, Re$k = q$.

cross any phase boundaries. Such a case is indeed materialized in the incommensurate-commensurate crossovers in the three-dimensional axial next-nearest-neighbor Ising (ANNNI) model [38,39] [which is of type (ii) in the classification above]. This phenomenon is also seen in the ground state phase diagram of Frenkel-Kontorova models [40] in which one of the coupling constants is tuned instead of temperature.

In the following, we present two alternative derivations for the universal exponent characterizing this crossover.

1. First approach

In general, if the pair correlation function $G(T,k)$ is a meromorphic function of the temperature T and the wave vector k near a crossover point (T_*,k_*), then $G^{-1}(T,k)$ must have a Taylor series expansion about that point. We have

$$G^{-1}(T,k) = \sum_{m_1,m_2=0}^{\infty} A_{m_1 m_2}(T-T_*)^{m_1}(k-k_*)^{m_2}. \quad (13)$$

Since $G^{-1}(T_*,k_*) = 0$, we have $A_{00} = 0$. In the simple canonical case, the leading order terms in Eq. (13) are given by

$$G^{-1} = A(T-T_*)^a + B(k-k_*)^b + \cdots \quad (14)$$

with a and b natural numbers and where A, B are constants.

We may examine the trajectory of the pole $K(T)$ of $G(T,k)$ [wherein $K(T_*) = k_*$] in the complex k plane as the temperature is varied around T_*. The case of Eq. (14) was written both for clarity and pedagogical purposes as well as its prevalence. In such a case, the pole K for which $G^{-1}(T,k=K) = 0$ will scale as

$$K(T) \sim k_* + C(T-T_*)^{a/b}, \quad (15)$$

where C is some constant, yielding $\nu_L = a/b$. There can, of course, be more interesting situations in which some number of mixed terms, all of which are products of powers of $(k-k_*)$ and $(T-T_*)$, are of the same order as $K(T)$ approaches k_*. In the general case, more interesting situations arise wherein some number of mixed terms in Eq. (13) [i.e., terms containing products of powers of both $(T-T_*)$ and $(k-k_*)$] are of the same order as $K(T)$ approaches k_*. After grouping the leading order terms, we will once again obtain Eq. (15) with some rational exponent (a/b).

By the very definition of T_*, on one side of T_* [(i) or (ii) above], there exists at least one root $K(T)$ of G^{-1} satisfying $K_R(T) = q$, where q is a constant. On the other side [(iii) above], $K_R(T) \neq q$. As such, the function $K(T)$ is nonanalytic at T_*. The left-hand side of Eq. (15) is therefore not analytic at $T = T_*$, implying that the right-hand side can not be analytic. This means that (a/b) can not be an integer, which in turn implies that $b \geqslant 2$. Therefore, in the most common situations we might encounter,

$$G^{-1}(T,k) \sim A(T-T_*) + B(k-k_*)^2 \Rightarrow a = 1 \text{ and } b = 2. \quad (16)$$

When Fourier transforming $G(T,k)$ by evaluating the integral in Eqs. (9) and (10) using the technique of residues, the real part of the poles (i.e., K_R) gives rise to oscillatory modulations of length $L_D = 2\pi/K_R$. If the modulation length locks its value to $2\pi/q$ on one side of the crossover point, then, on the other side, near T_*, it must behave as

$$|2\pi/L_D - q| \propto |T-T_*|^{1/2} \Rightarrow \boxed{\nu_L = 1/2.} \quad (17)$$

2. Second approach

We now turn to a related alternative approach that similarly highlights the universal character of the modulation length exponent. If the correlation function $G(T,k)$ is a meromorphic function of k, then, expanding about a zero $K_1(T)$ of G^{-1}, we have

$$G^{-1}(T,k) = A(T)[k-K_1(T)]^{m_1} G_1^{-1}(T,k), \quad (18)$$

where $G_1^{-1}(T,k)$ is an analytic function of k and $G_1^{-1}[T,K_1(T)] \neq 0$. We can do this again for the function $G_1^{-1}(T,k)$, choosing one of its zeros $K_2(T)$, and continue the process until the function left over does not have any more zeros. We have

$$G^{-1}(T,k) = A(T)\prod_{a=1}^{p}[k-K_a(T)]^{m_a} G_p^{-1}(T,k), \quad (19)$$

where the function $G_p^{-1}(T,k)$ is an analytic function with no zeros, m_a's are integers, and, in principle, p may be arbitrarily high. This factorization can be done in each phase where G is meromorphic. Let $K_1(T)$ be a nonanalytic zero of G^{-1}, i.e., one for which $\mathrm{Re}K_1(T) = q$ on one side of $T = T_*$. To ensure analyticity of G^{-1} in T in the vicinity of $T = T_*$, there must be at least one other root $K_2(T)$, such that as $T \to T_*$, both $K_1(T)$ and $K_2(T)$ veer towards k_*, where $\mathrm{Re}k_* = q$ [e.g., see Fig. 3 which is of type (i) above, $k_* = \pm i$]. In other words, p in Eq. (19) can not be smaller than two. The proof of this assertion

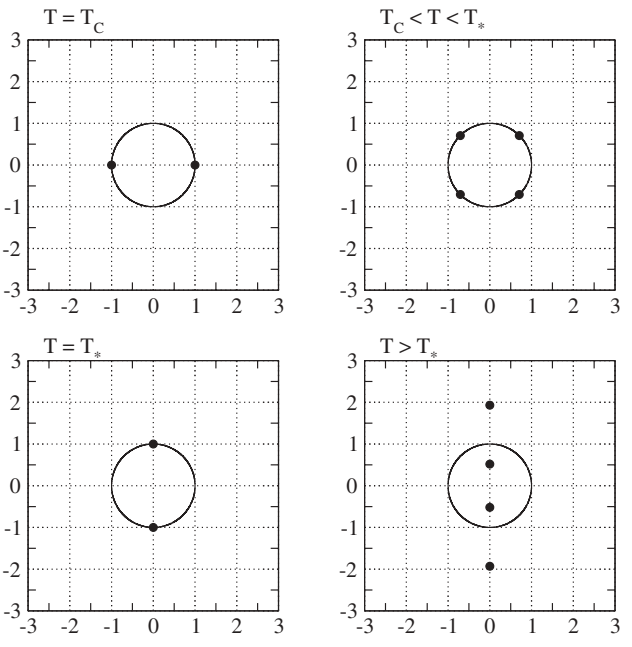

FIG. 3. Location of the poles of the correlation function of the large n Coulomb frustrated ferromagnet for $J = Q = 1$ in the complex k plane. The circle and the Y axis show the trajectory $K(T)$ of the poles as the temperature T is varied.

is simple. If $p = 1$, then, according to Eq. (19), $G^{-1}(T,k) = A[k - K_1(T)]G_1^{-1}(T,k)$. At $T = T_*$, however, $K_1(T)$ is not analytic, implying that $G^{-1}(T,k)$ can be analytic only if $p \geqslant 2$. For $p \geqslant 2$, at T_*, G^{-1} will, to leading order, vary quadratically in $(k - k_*)$ in the complex k plane near k_*. Thus,

$$\left.\frac{\partial G^{-1}}{\partial k}\right|_{(T_*,k_*)} = 0. \tag{20}$$

Now, if G^{-1} has a finite first partial derivative relative to the temperature T, then, for a pole K near k_* to leading order

$$G^{-1}(T_*,k_*) + (T - T_*)\left.\frac{\partial G^{-1}}{\partial T}\right|_{(T_*,k_*)} + \frac{(K - k_*)^2}{2!}\left.\frac{\partial^2 G^{-1}}{\partial k^2}\right|_{(T_*,k_*)} = 0. \tag{21}$$

By its definition, k_* satisfies the equality $G^{-1}(T_*,k_*) = 0$. Therefore,

$$|K - k_*| = \sqrt{\frac{2(T_* - T)\left.\frac{\partial G^{-1}}{\partial T}\right|_{(T_*,k_*)}}{\left.\frac{\partial^2 G^{-1}}{\partial k^2}\right|_{(T_*,k_*)}}}. \tag{22}$$

Equation (17) is an exact equality. It demonstrates that the exponent $\nu_L = 1/2$ *universally* unless one of $\frac{\partial^2 G^{-1}}{\partial k^2}$ and $\frac{\partial G^{-1}}{\partial T}$ vanishes at (T_*,k_*) [41]. Often, $G^{-1}(T,k)$ is a rational function of k, i.e.,

$$G^{-1}(T,k) = \frac{G_n^{-1}(T,k)}{G_d^{-1}(T,k)}, \tag{23}$$

where $G_n^{-1}(T,k)$ and $G_d^{-1}(T,k)$ are polynomial functions of k. In those instances, we get the same result as above by using $G_n^{-1}(T,k)$ in the above arguments. The value of the modulation length exponent is similar to that appearing for the correlation length exponent for mean-field or large n theories. It should be stressed that our result of Eq. (17) is far more general.

B. Lock-in of the correlation length

Apart from the crossovers across which the modulation length locks in to a fixed value, we can also have situations where the correlation length becomes constant as a crossover temperature T_{**} is crossed. If this happens, our earlier analysis for the modulation length may be replicated anew for the correlation length. Therefore, if the correlation length has a fixed value ξ_0 on one side ($T < T_{**}$ or $T > T_{**}$) of the crossover point, then, on the other side ($T > T_{**}$ or $T < T_{**}$, respectively), near T_{**} it must behave as

$$|1/\xi - 1/\xi_0| \propto |T - T_{**}|^{\nu_c}, \tag{24}$$

where, like ν_L, $\nu_c = 1/2$ apart from special situations where it may take some other rational values. Here and throughout, we use ν_c to represent the usual correlation length exponent ν to distinguish it from the modulation length exponent ν_L.

C. Exponents in parity invariant systems associated with real (or imaginary) poles

Our results of Secs. IV A1 and IV A2 pertained to general crossovers associated with general wave vectors. A simplification occurs in parity (or reflection) invariant systems with real spatial correlation functions, when either the real or imaginary parts of the poles of the correlation function vanish (i.e., $K_I = 0$ or $K_R = 0$). In this case, we can reobtain the results of Secs. IV A1 and IV A2 along an alternate route as we now illustrate.

As is well known, whenever the spatial pair correlation functions $G(T,\vec{x})$ are real, a Fourier transform about the lth direction yields

$$G(T,\{x_{l'\neq l}\},-k_\ell) = G^*(T,\{x_{l'\neq l}\},k_l), \tag{25}$$

with G^* the complex conjugate of G. Furthermore, in systems with an invariance associated with a reflection about the lth Cartesian direction,

$$G(T,\{k_{l'\neq l}\},k_l) = G(T,\{k_{l'\neq l}\},-k_l). \tag{26}$$

Taken together, Eqs. (25) and (26) imply that if, for a fixed value of $\{x_{l'\neq l}\}$, G as a function of k_l has a pole at K, then it must also have poles at $\{-K,K^*,-K*\}$. In rotationally invariant systems, $G(T,\vec{k})$ is a function of k^2 (k is the modulus of the wave vector $\vec{k}$) and similar results hold. That is, if $G(k)$ has a pole at K, then it also has poles at $\{-K,K^*,-K^*\}$.

We now consider two situations.

1. The crossover is associated with k_* that lies on the imaginary axis in the complex k plane

In this case, by virtue of the above considerations, as a pole K veers towards k_* so must its counterpart $-K^*$ (which as illustrated above is also a pole of G). Thus, in expanding $G^{-1}(T,k_l)$ or $G(T,k)$ (with $k^2 = \vec{k}\cdot\vec{k}$) about the zero at k_* and $T = T_*$, we have, exactly as in Eq. (16),

$$G^{-1} \sim A(T - T_*) + B(k - k_*)^{2s}, \tag{27}$$

with $s = 1$ and where A, B are constants. In such a case, as in our earlier discussion, the modulation length diverges at $T = T_*$ with an exponent of $\nu_L = 1/2$. [The size of the modulation length scales as the reciprocal of the absolute value of the real part ($|K_R|$) of K.] It is, of course, also possible to have any even number ($2s$) of pairs of momenta $\{K, -K^*\}$ in the complex k plane converging on $k = k_*$ at $T = T_*$. In such instances, the modulation length diverges:

$$\nu_L = \frac{1}{2s}. \tag{28}$$

2. The crossover is associated with k_* that lies on the real axis in the complex k plane

Here, invoking anew the results that stem from Eqs. (25) and (26), we have that as a pole K of G veers towards a real k_*, so does the pole K^* of G. Replicating the considerations above, we arrive at Eq. (27) once again. The point k_* on the real axis is associated with a diverging correlation length [whose size scales as the reciprocal of the absolute value of the imaginary part ($|K_I|$) of K]. Similar to Eq. (28), the correlation length exponent ν_c associated with this crossover will be given by

$$\nu_c = \frac{1}{2s} \tag{29}$$

with s a natural number.

D. Branch points

A general treatment of a situation in which the crossover point is a branch point of the inverse correlation function in the complex k plane is beyond the scope of this work. Branch points are ubiquitous in correlation functions in both classical as well as quantum systems.

For example, in the large n rendition of a bosonic system [with a Hamiltonian of Eq. (3) and $S(x)$ representing bosonic fields], the momentum space correlation function at temperature T is given by Refs. [35,42]

$$G(\vec{k}) = \sqrt{\frac{\mu_1}{v(\vec{k})+\mu}}\left[n_B\left(\frac{\sqrt{\mu_1[v(\vec{k})+\mu]}}{k_B T}\right)+\frac{1}{2}\right], \quad (30)$$

where μ_1 is a constant having dimensions of energy, μ is the chemical potential, $n_B(x) = 1/(e^x - 1)$ is the Bose distribution function, and k_B is Boltzmann's constant.

Similar forms, also including spatial modulations in $G(r)$, may also appear. We briefly discuss examples where we have a branch cut in the complex k plane.

The one-dimensional momentum space correlation function

$$G(k) = \frac{1}{\sqrt{(k-q)^2+r}} + \frac{1}{\sqrt{(k+q)^2+r}} \quad (31)$$

reflects a real space correlation function given by

$$G(x) = \frac{2\cos(qx)\mathrm{K}_0(x\sqrt{r})}{\pi}, \quad (32)$$

where $\mathrm{K}_0(\ldots)$ is a modified Bessel function. Thus, as is to be expected, we obtain length scales associated with the branch points $K = \pm q \pm i\sqrt{r}$.

Similarly, the three-dimensional real space correlation function corresponding to

$$G(k) = \frac{1}{\sqrt{(k-q)^2+r}} \quad (33)$$

exhibits the same correlation and modulation lengths along with an algebraically decaying term for large separations. Another related $G^{-1}(k)$ involving a function of $|\vec{k}|$ (i.e., not an analytic function of k^2) was investigated earlier [43].

Throughout the bulk of our work, we consider simple exponents associated with analytic crossovers. In considering branch points, our analysis may be extended to critical points. As is well known, at critical points of d-dimensional systems, the correlation function for large r scales as

$$G(r) \propto \frac{1}{r^{d-2+\eta}}, \quad (34)$$

with η the *anomalous* exponent. Such a scaling implies, for noninteger η, the existence of a branch point of $G(k)$ at $k = 0$.

If the leading order behavior of $1/G^{(m)}(T,k)$ is algebraic near a branch point (T_*,k_*), then we get an algebraic exponent characterizing a crossover at this point [m being the lowest order derivative of $G(k)$ which diverges at $k = k_*$ as in Eq. (12)]. That is, we have

$$\frac{1}{G^{(m)}(T,k)} \sim A(T-T_*)^{z_1} - B(k-k_*)^{z_2} \quad \text{as } (T,k) \to (T_*,k_*), \quad (35)$$

with some constants A and B. This implies that the branch points K deviate from k_* as

$$(K-k_*) \sim \left(\frac{A}{B}\right)^{1/z_2}(T-T_*)^{z_1/z_2}. \quad (36)$$

We therefore observe a length scale exponent $\nu = z_1/z_2$ at this crossover. This exponent may characterize a correlation length and/or a modulation length. The exponent z_1/z_2 may assume *irrational* values in many situations in which the function $G^{-1}(T,k)$ is not analytic near the crossover point. Such a situation could give rise to phenomena exhibiting anomalous exponents η. For example, if we have a diverging correlation length at a critical temperature T_c for a system with a correlation function which behaves as in Eq. (34), then we have in Eq. (35) $z_2 = 2 - \eta$. Thus, we have

$$|L_D - L_{Dc}| \propto |T-T_c|^{\frac{z_1}{2-\eta}} \Rightarrow \boxed{\nu_L = \frac{z_1}{2-\eta}}, \quad (37)$$

where $L_{Dc} = 2\pi/|\mathrm{Re}k_*|$, and more importantly

$$\xi \propto |T-T_c|^{-\frac{z_1}{2-\eta}} \Rightarrow \boxed{\nu_c = \frac{z_1}{2-\eta}}. \quad (38)$$

Other critical exponents could also, in principle, be calculated using hyperscaling relations.

If $G^{-1}(T,k)$ has a Puiseux representation about the crossover point, i.e.,

$$G^{-1}(T,k) = \sum_{m=m_0}^{\infty}\sum_{p=p_0}^{\infty} a_{mp}(k-k_*)^{m/a}(T-T_*)^{p/b}, \quad (39)$$

with $a_{m_0p_0} = 0$, where m_0, p_0, a, and b are integers, then, the result we derived above applies to the relevant length scale and the crossover exponent $\nu = a/b$ is again a *rational number*. Generalizing, if $G^{-1}(T,k)$ is the ratio of two Puiseux series, we use the numerator to obtain the leading order asymptotic behavior and hence obtain a rational exponent.

E. A corollary: Discontinuity in modulation lengths implies a thermodynamic phase transition

Nonanalyticities in the correlation function $G(k)$ for a real wave vector k imply the existence of a phase transition. This leads to simple corollaries as we now briefly elaborate on. A sharp discontinuous jump in the value of the modulation lengths (and/or correlation lengths) implies that the zeros $\{K_a\}$ of $G^{-1}(k)$ in the complex k plane exhibit discontinuous ("first-order-like") jumps as a function of some parameter (such as the temperature T). When this occurs, as seen by, e.g., differentiating the reciprocal of the product of Eq. (19), the correlation function will, generally, not be analytic as a function of T at $T = T_*$. Putting all of the pieces together, we see that a discontinuous change in the modulation (or correlation) lengths implies the existence of a bona fide phase transition. Thus, all commensurate-commensurate crossovers must correspond to phase transitions. An example is afforded by the ANNNI model [44].

F. Diverging correlation length at a spinodal transition

Our analysis is valid for both annealed and quenched systems so long as translational symmetry is maintained (and thus, the correlation function is diagonal in k space). In particular, whenever phase transitions are "avoided," the rational exponents of Eq. (15) will appear [42,45,46].

In diverse arenas, we may come across situations in which there are no diverging correlation lengths even when the inverse correlation function has zeros corresponding to real values of the wave vector. These are signatures of a first-order phase transition, e.g., transition from a liquid to a crystal. If the first-order phase transition is somehow avoided, then the system may enter a metastable phase and may further reach a point where the correlation length diverges, e.g., a spinodal point. If it is possible to reach this point and if the inverse correlation function is analytic there, then our analysis will be valid, thereby leading to rational exponents characterizing the divergence of the correlation length. There are existing works in the literature which seem to suggest that such a point may not be reachable. For example, in mode coupling theories of the glass transition, the system reaches the mode coupling transition temperature $T_{\rm MCT}$, at which the viscosity and relaxation times diverge and the system does not reach the point where the correlation length blows up [47].

G. Conservation of total number of characteristic length scales

In Ref. [35], it was mentioned that the total number of characteristic length scales in a large n system remains constant in systems in which the Fourier space interaction kernel $v(\vec{k})$ is a rational function of k^2 and the real space kernel is rotationally invariant. (Similar results hold for systems with reflection point group symmetry [48].) In this section, we generalize that argument and say that whenever the Fourier space correlator $G(\vec{k})$ of a general rotationally invariant system is a rational function of k^2, i.e.,

$$G(\vec{k}) = \frac{P(k^2)}{Q(k^2)}, \tag{40}$$

the total number of correlation and modulation lengths remains constant apart from isolated points as a tuning parameter λ is smoothly varied. In Eq. (40), the functions $P(k^2)$ and $Q(k^2)$ are polynomial functions of k^2. Rotational invariance requires that $G(\vec{k})$ is real valued for real wave vectors k. As argued in Ref. [35], all length scales in the such systems are associated with the poles of $G(k)$ in the complex k plane and these remain constant for a given form of the function $G(k)$. Each real root of the function $Q(k^2)$ gives rise to a term in the real space correlation function, which has one correlation or one modulation length. Nonreal roots (which necessarily come in complex conjugate pairs) give rise to a correlation and a modulation length. Thus, the total number of characteristic length scales in the system is equal to the order of the polynomial function $Q(k^2)$ which remains fixed.

V. $O(n)$ SYSTEMS

The correlation function for $O(n)$ systems can be calculated exactly at both the low and the high temperature limits. At intermediate temperatures, various crossovers and phase transitions may appear. In this section, we discuss the low and high temperature behavior length scales characterizing $O(n)$ systems.

A. Low temperature configurations

It was earlier demonstrated [49] that for $O(n \geqslant 2)$, *all* ground states of a system have to be spirals (or polyspirals) of characteristic wave vectors $\vec{q}_\alpha$, given by

$$v(\vec{q}_\alpha) = -\min_{\vec{k}\in\mathbb{R}^d} v(\vec{k}), \tag{41}$$

where $\mathbb{R}^d$ represents the set of all d-dimensional real vectors. At $T = 0$, the modulation lengths in the system are given by

$$L_D^{i,\alpha}(T=0) = 2\pi/q_{i,\alpha}, \tag{42}$$

where $i (1 \leqslant i \leqslant d)$ labels the Cartesian directions in d dimensions. This, together with Eq. (43), gives us the high and low temperature forms of the correlation function and its associated length scales.

B. High temperatures

As is well appreciated, diverse systems behave in the same way at high temperatures [50]. For $O(n)$ systems [51] (any n),

$$G^{-1}(T,k) = 1 + v(\vec{k})/k_BT + \mathcal{O}(1/T^3). \tag{43}$$

The high temperature series may be extended and applied at the crossover temperature T_* if there is no phase transition at temperatures above T_* and for all relevant real k's, $|v(\vec{k})| \ll k_BT_*$. (A detailed example will be studied in Sec. V E.) Generally, Eq. (43) may be analytically continued for complex k's and in the vicinity of T_*:

$$\delta k \sim \left[\frac{m!k_B(T_*-T)}{v^{(m)}(k_*)}\right]^{\frac{1}{m}}, \tag{44}$$

where k_* is a characteristic wave vector at T_*. In the above, δk denotes the change in the location of the poles K of G^{-1} when the temperature is changed from T_* to T (i.e., $\delta k \equiv K - k_*$) and m is the order of the lowest nonvanishing derivative of $v(\vec{k})$ at k_*. As in previous analysis, $v'(k_*) = 0$ and $m \geqslant 2$. For general $v(\vec{k})$, typically $m = 2$ and $\nu_L = 1/2$ as before.

We now turn to examples which explicitly illustrate how our results are realized including exceptional systems with nontrivial exponents.

C. Large n Coulomb frustrated ferromagnet: Modulation length exponent at the crossover temperature T_*

In this section and the two that follow, we will discuss the large n limit in $O(n)$ systems. The results in the previous two sections pertain to arbitrary n. We illustrate how our result applies to the large n [51] Coulomb frustrated ferromagnet. As is well known [52], in the large n limit, $O(n)$ systems are exactly solvable and behave as the spherical model [53]. The correlation function in k space is given by

$$G^{-1}(T,k) = [v(\vec{k}) + \mu(T)]/k_BT, \tag{45}$$

where $v(\vec{k})$ is the Fourier space interaction kernel and $\mu(T)$ is a Lagrange multiplier (see e.g. Refs. [35,46]) that enforces the

spherical constraint

$$\frac{1}{N}\sum_{\vec{x}}\langle\vec{S}(\vec{x})\cdot\vec{S}(\vec{x})\rangle = 1. \tag{46}$$

The paramagnetic transition temperature T_C is obtained from the relation $\mu(T_C) = -\min_{k\in\mathbb{R}} v(\vec{k})$. Below T_C, the Lagrange multiplier $\mu(T) = \mu(T_C)$. Above T_C, $\mu(T)$ is determined by the global average constraint that $G(\vec{x}=0) = \frac{1}{N}\sum_{\vec{k}} G(\vec{k})$=1. This global constraint also implies that, above T_C, small changes in temperature result in proportional changes in $\mu(T)$ and at high temperatures, $\mu(T)$ is a monotonic increasing function of T. The Fourier space kernel $v(\vec{k})$ for the "Coulomb frustrated ferromagnet" (in which nearest-neighbor ferromagnetic interactions of strength J compete with Coulomb effects of strength Q) is given by $v(\vec{k}) = Jk^2 + Q/k^2$, where J and Q are positive constants. The critical temperature T_C of this system is given by $\mu(T_C) = -2\sqrt{JQ}$. At T_C, the correlation length is infinity and the modulation length is $L_D = 2\pi\sqrt[4]{J/Q}$. As the temperature is increased, the modulation length increases and the correlation length decreases. At T_*, given by $\mu(T_*) = 2\sqrt{JQ}$, the modulation length diverges and the correlation length becomes $\xi = \sqrt[4]{J/Q}$. At temperatures above T_*, the correlation function exhibits no modulations and there is one decreasing correlation length and one increasing correlation length. The term in the correlation function with the increasing correlation length becomes irrelevant at high temperatures because of an algebraically decaying prefactor. The divergence of the modulation length at T_* shows an exponent of $\nu_L = 1/2$ [35].

D. An example with $\nu_L \neq 1/2$

In what follows, we demonstrate, as a matter of principle, that the exponent for the divergence of the modulation length (and also the correlation length) can be different from 1/2 in certain special cases. As an illustrative example, we consider a large n (or spherical model) system for which, in Eq. (6),

$$v(\vec{k}) = A\left(k^2 + l_s^{-2}\right)^2 + 4B\left(k^2 + l_s^{-2}\right) + 4C/\left(k^2 + l_s^{-2}\right) + D/\left(k^2 + l_s^{-2}\right)^2, \tag{47}$$

where l_s is a screening length and A, B, C, D are constants. If we set $A = B = C = D = 1$, then in the resultant system $\nu_L \neq 1/2$ at a crossover temperature. It has a critical temperature T_C, given by $\mu(T_C) = -10$. At T_C, the modulation length is $L_D = 2\pi/\sqrt{1 - 1/l_s^2}$ and the correlation length blows up (as required by definition). At the crossover temperature, T_* [for which $\mu(T_*) = 6$], the modulation length diverges and the correlation length scales as $\xi = 1/\sqrt{1 + 1/l_s^2}$. A temperatures just below T_*, the modulation length L_D diverges as $L_D \propto (T_* - T)^{-1/4}$, meaning that $\nu_L = 1/4$. This is because the first three derivatives of $v(\vec{k})$ vanish at $k = i$, which is the characteristic wave vector at T_* (see Fig. 4).

E. An example in which T_* is a high temperature

We now provide an example in which the high temperature result of Sec. V B [valid for any $O(n)$ system with arbitrary n] can be applied at a crossover point. Consider the large n system in Eq. (47) with $A = 1$, $B \gg 1$, $C = 1/4$, $D = 0$,

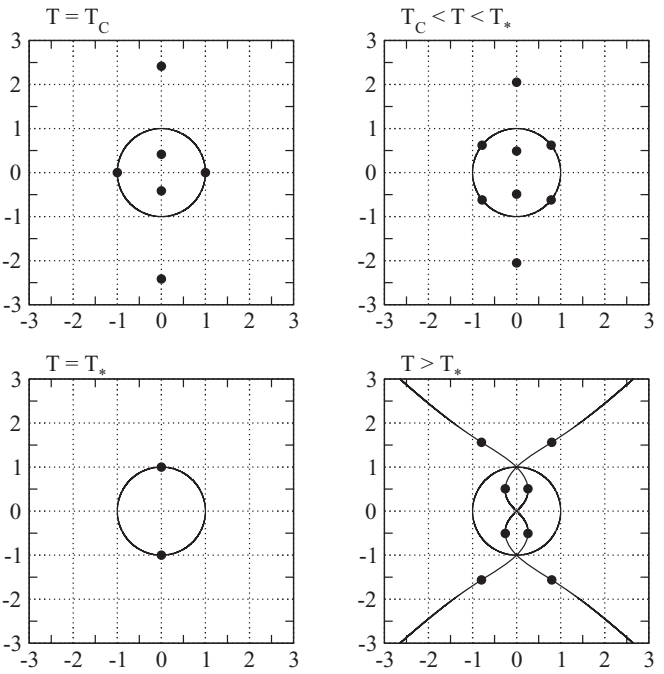

FIG. 4. Location of the poles of the correlation function of the system in Eq. (47) for large l_s (small screening) in the complex k plane.

and the screening length $l_s \gg B$. The critical temperature of this system is given by $\mu(T_C) \sim -4\sqrt{B}$ where the modulation length is $L_D \sim 2\pi\sqrt[4]{4B}$. There is a crossover temperature T_* such that $\mu(T_*) \sim 4B^2$. One of the modulation lengths diverges at T_*. The corresponding correlation length is given by $\xi \sim 1/\sqrt{2B}$. This provides an example in which $|v(\vec{k})| \ll k_B T_*$ for all real k's satisfying $|k| \leqslant \pi$. The second derivative of $v(\vec{k})$ is nonzero at the crossover point, resulting in a crossover exponent $\nu_L = 1/2$.

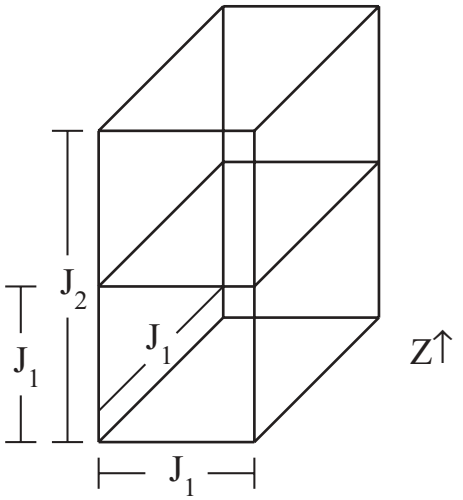

FIG. 5. The coupling constants in the three-dimensional ANNNI model.

VI. CROSSOVERS IN THE ANNNI MODEL

We now comment on one of the oldest studied examples of a system with a crossover temperature. The following Hamiltonian represents the axial next-nearest-neighbor Ising (ANNNI) model [38,39,44]:

$$H = -J_1 \sum_{\langle \vec{x},\vec{y}\rangle} S(\vec{x})S(\vec{y}) + J_2 \sum_{\langle\langle \vec{x},\vec{y}\rangle\rangle} S(\vec{x})S(\vec{y}), \qquad (48)$$

where, as throughout, $\{\vec{x}\}$ is a cubic lattice, and the (Ising) spins $S(\vec{x}) = \pm 1$. The couplings $J_1, J_2 > 0$. In the summand, $\langle \ldots \rangle$ represents nearest neighbors and $\langle\langle \ldots \rangle\rangle$ represents next-nearest neighbors along one axis (say the Z axis) (see Fig. 5). Depending on the relative strength J_2/J_1, the ground state may be either ferromagnetic or in the "$\langle 2 \rangle$ phase." The "$\langle 2 \rangle$ phase" is a periodic layered phase, in which there are layers of width two lattice constants of "up" spins alternating with layers of "down" spins of the same width along the Z axis. As the temperature is increased, the correlation function exhibits jumps in the modulation wave vector at different temperatures. At these temperatures, the system undergoes first-order transitions to different commensurate phases. The inverse correlation function $G^{-1}(T,k)$ is therefore not an analytic function of k and T at the transition points. The phase diagram for the ANNNI model, however, also has several crossovers where the system goes from a commensurate phase to an incommensurate phase with a continuously varying modulation length (see Fig. 6) [54,55]. At these crossover points, following our rigorous analysis, we expect a crossover exponent $\nu_L = 1/2$. Such a scaling of the modulation length has been estimated by several approximate techniques near the "Lifshitz point" P_L [44,56–61]. The Lifshitz point is the point in the phase diagram of the ANNNI model at which the high temperature paramagnetic phase coexists with the

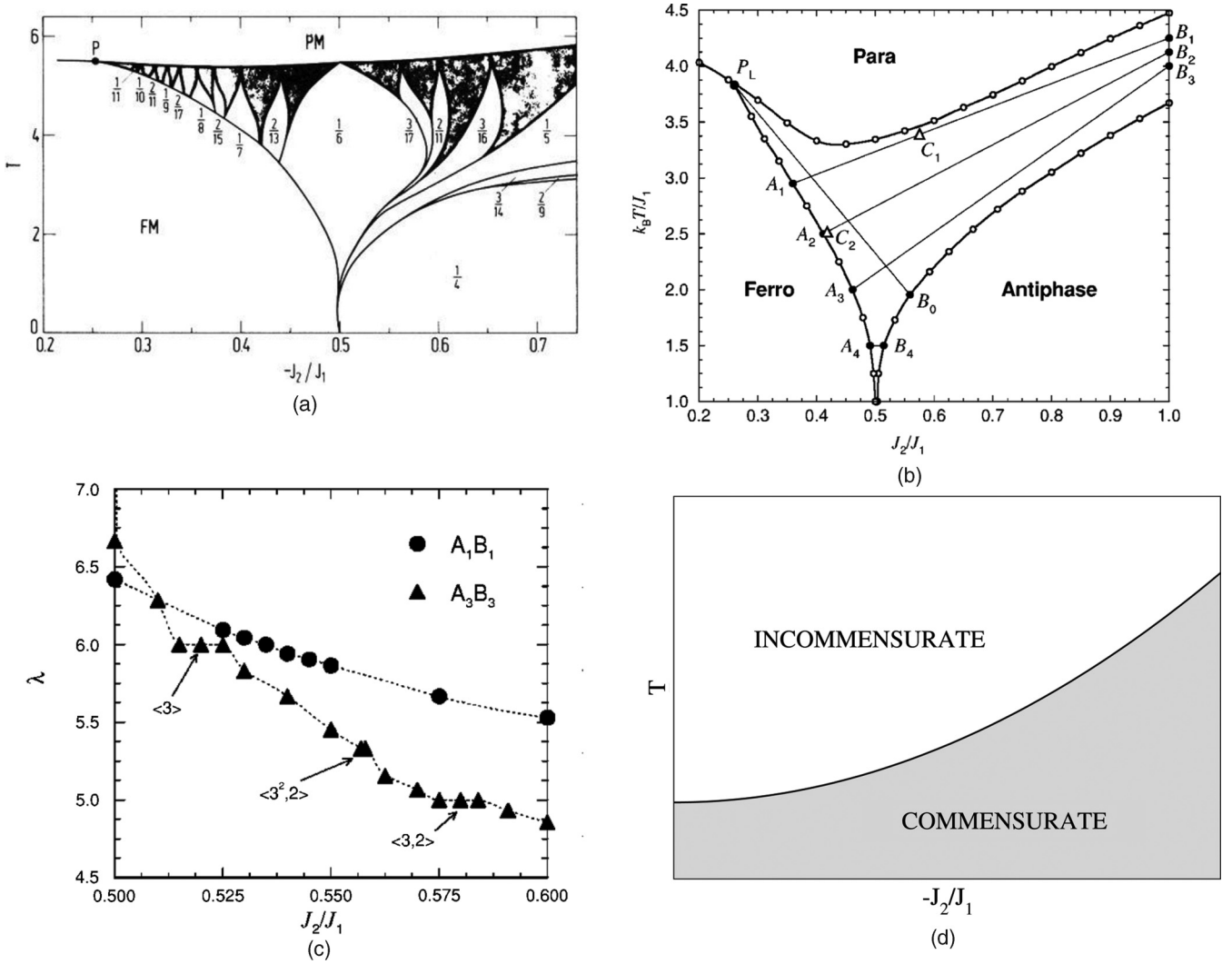

FIG. 6. Existence of incommensurate phases between the commensurate regions in the phase diagram of the ANNNI model. (a) Mean-field phase diagram of the ANNNI model in three dimensions. The shaded regions show higher order commensurate phases which have variable modulation length incommensurate phases in-between. (From Ref. [54], reprinted with permission from APS.) (b) Phase diagram for the three-dimensional ANNNI model using a modified tensor product variational approach. (From Ref. [55], reprinted with permission from APS.) (c) Variation of wavelength along paths A_1B_1 and A_3B_3 of (b) showing a smooth variation of the wavelength near the paramagnetic transition line. (From Ref. [55], reprinted with permission from APS.) (d) Cartoon of an incommensurate-commensurate crossover region from (a).

ferromagnetic phase as well as a phase with continuously varying modulation lengths. It is marked as P_L in Fig. 6(b). Although the point P_L has a first-order transition, it can be thought of as a limit in which the incommensurate and commensurate regions in Fig. 6(a) shrink and merge to a single point. We would also like to point out that it is known [62] that if the wave vector takes all possible rational values ("complete devil's staircase"), we have no first-order transitions. Additionally, nonanalyticity of the correlation function does not prohibit other quantities from having continuous crossover behavior. For example, the correlation of the fluctuations, i.e., the connected correlation function may generally exhibit continuous variation from a fixed to a variable modulation length phase. If the inverse connected correlation function is analytic, our result can be applied to it, resulting in a crossover exponent of $1/2$.

Aside from its theoretical appeal, the ANNNI model has numerous applications and natural generalizations. We note that aside from the spin only ANNNI Ising exchange Hamiltonian of Eq. (48), it is notable that, inspired by experimental results, much work has further focused on the effects of additional applied magnetic field that augment such bare spin exchange interactions [63,64].

VII. PARAMETER EXTENSIONS AND GENERALIZATIONS

It is illuminating to consider simple generalizations of our result to other arenas. We may also replicate the above derivation for a system in which, instead of temperature, some applied other field λ is responsible for the changes in the correlation function of the system. Some examples could be pressure, applied magnetic field, and so on. The complex wave vector k could also be replaced by a frequency ω, the imaginary part of which would then correspond to some decay constant in the time domain.

More generally, we look for solutions to the equation

$$G^{-1}(\lambda,u) = 0, \tag{49}$$

with the variable u being a variable Cartesian component of the wave vector, the frequency, or any other momentum space coordinate appearing in the correlation function between two fields ($u = k_i, \omega$, and so on). Replicating our steps *mutatis mutandis*, we find that the zeros of Eq. (49) scale as $|u - u_0| \propto |\lambda - \lambda_*|^{1/2}$ whenever the real (or imaginary) part of some root becomes constant as λ crosses λ_*. Thus, our predicted exponent of $\nu_L = 1/2$ could be observed in a vast variety of systems in which a crossover occurs as the applied field crosses a particular value, in the complex wave-vector-like variable.

Another generalization of our result proceeds as follows [65]. Suppose that we have a general *analytic* operator (including any inverse propagator) $G^{-1}(\lambda)$ that depends on a parameter λ. Let a_α be a particular eigenvalue

$$G^{-1}(\lambda)|a_\alpha(\lambda)\rangle = a_\alpha(\lambda)|a_\alpha(\lambda)\rangle. \tag{50}$$

The secular equation for the eigenvalues of G^{-1} is an analytic function in λ. We may thus replicate our earlier considerations to obtain similar results. In doing so, we see that if $a_\alpha(\lambda)$ changes from being purely real to becoming complex as we vary the parameter λ beyond a particular threshold value λ_* [i.e., if $a_\alpha(\lambda > \lambda_*)$ is real and $a_\alpha(\lambda < \lambda_*)$ is complex, or vice versa], then the imaginary part of $a_\alpha(\lambda)$ will scale (for $\lambda < \lambda_*$ in the first case noted above and for $\lambda > \lambda_*$ in the second one) as $\mathrm{Im}\,\{a_\alpha(\lambda)\} \propto |\lambda - \lambda_*|^{1/2}$. A particular such realization is associated with the spectrum of a non-Hermitian Hamiltonian [playing the role of G^{-1} in Eq. (50)] which, albeit being non-Hermitian, may have real eigenvalues (as in $\mathcal{PT}$ symmetric Hamiltonians) [66]. In this case, the crossover occurs when a system becomes $\mathcal{PT}$ symmetric as a parameter λ crosses a threshold λ_*.

Similarly, if $a_\alpha(\lambda)$ changes from being pure imaginary to complex at $\lambda = \lambda_*$, then the real part of the eigenvalue will scale in the same way. That is, in the latter instance, $\mathrm{Re}\,\{a_\alpha(\lambda)\} \propto |\lambda - \lambda_*|^{1/2}$.

Our next brief remark pertains to some theories with multicomponent fields, e.g., n component theories with Hamiltonians of the form Ref. [42]

$$H = \frac{1}{2N}\sum_{\vec{k},i,j} v_{ij}(k) s_i(\vec{k}) s_j(\vec{k}), \tag{51}$$

in which, unlike Eq. (6) [as well as standard $O(n)$ theories], the interaction kernel v_{ij} might not be diagonal in the internal field indices $i,j = 1,2,\ldots,n$. An example is afforded by a field theory in which n component fields are coupled minimally to a spatially uniform (and thus translationally invariant) non-Abelian gauge background which emulates a curved space metric [42]. Due to the density of states of this system, an exact dimensional reduction occurs at low energies [67]. In the large n system of Eq. (51), the index α in Eq. (50) is a composite of an internal field component coordinate $w = 1,2,\ldots,n$ and $\vec{k}$-space coordinates. For each of the n branches w, we may determine the associated $\vec{k}$-space zero eigenvalue of Eq. (50) which we label by K_w [i.e., $a_{w,k=K_w}(\lambda) = 0$]. The largest correlation length is associated with the eigenvector which exhibits the smallest value of $|\mathrm{Im}K_w|$. As usual, as λ is varied, we may track for each of the n branches the trajectories poles of G in the complex k plane. Although the location of the multiple poles may vary continuously with the parameter λ, the dominant poles (those associated with the largest correlation length) might discontinuously change from one particular subset of eigenvectors to another (see Fig. 7). As such, the correlation function of the system may show jumps in its dominant modulation length at large distances as λ crosses a threshold value λ_* even though no transitions (nor crossovers similar to that of Fig. 2 which form the focus of this work) are occurring. Such jumps in the large distance modulation lengths indeed appear in $O(n)$ systems defined on a fixed, translationally invariant, non-Abelian background or metric as in Ref. [42].

In Appendix A, we discuss exponents associated with lock-ins of correlation and modulation lengths in Fermi systems. When dealing with zero temperature behavior, we use the chemical potential μ as the control parameter λ. We discuss metal-insulator transition, exponents in Dirac systems, and topological insulators. Additionally, we comment on crossovers related to changes in the Fermi surface topology as well as those related to situations with divergent effective mass.

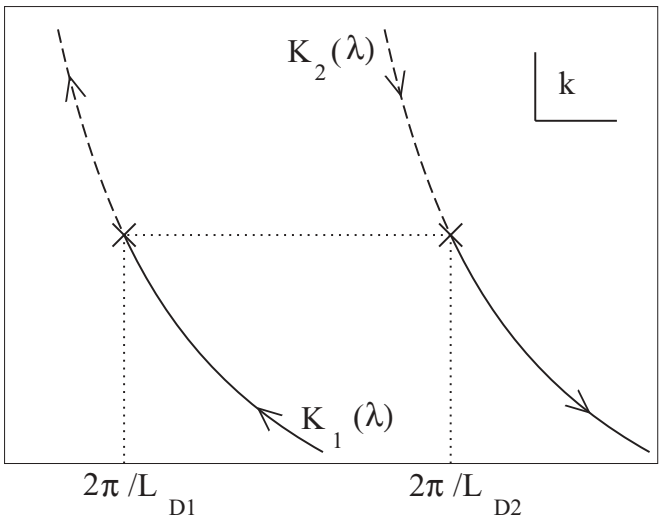

FIG. 7. "Jumps" in the modulation length: The figure shows the evolution of the poles associated with two different eigenvectors with the parameter λ in the complex k plane. The solid portions of the trajectories show which pole corresponds to the dominant term (larger correlation length) in the correlation function. The $\times$'s denote the poles at $\lambda = \lambda_*$ and the arrows denote the direction of increasing λ. It is evident, therefore, that the modulation length corresponding to the dominant term jumps from L_{D1} to L_{D2} as λ crosses the threshold value λ_*.

VIII. IMPLICATIONS FOR THE TIME DOMAIN: JOSEPHSON TIME SCALES AND RESONANCE LIFETIMES

As we alluded to above, the results that we derived earlier that pertained to length scales can also be applied to time scales in which case we look at a temporal correlation function characterized by decay times (corresponding to correlation lengths) and oscillation periods (corresponding to modulation lengths). We may obtain decay time and oscillation period exponents whenever one of these time scales freezes to a constant value as some parameter λ crosses a threshold value λ_*.

Many other aspects associated with length scales have analogs in the temporal regime. Towards this end, in what follows, we advance the notion of a "Josephson time scale." We first very briefly review below the concept of a Josephson length scale. In many systems [with correlation functions similar to Eq. (34)], just below the critical temperature, the correlation function as a function of wave vector k behaves as

$$G(k) \propto \begin{cases} k^{-2+\eta} & \text{for} \quad k \gg 1/\xi_J, \\ k^{-2} & \text{for} \quad k \ll 1/\xi_J, \end{cases} \tag{52}$$

thus defining the Josephson length scale ξ_J [68]. Such an argument may be extended to a time scale τ_J (real or imaginary) in systems with Lorentz invariant propagators. For a given wave vector k, τ_J may be defined as

$$G(k,\omega) \propto \begin{cases} \omega^{-2+\eta_t} & \text{for} \quad \omega \gg 1/\tau_J, \\ \omega^{-2} & \text{for} \quad \omega \ll 1/\tau_J, \end{cases} \tag{53}$$

where ω is the frequency conjugate to time while performing the Fourier transform and $\eta_t (\neq 0)$ is an anomalous exponent for the time variable.

We next briefly allude to another possible simple application of our result. As is well known in high energy (see, e.g., Ref. [69] for a standard textbook treatment) and many body theories, the Fourier transform of the two-point correlation function $G(\vec{k},\omega)$ generally exhibits isolated poles corresponding to the one-particle states as well as bound states and a branch cut that reflects a continuum of multiparticle states (i.e., two particles or more). Such a continuum of states arises when the squared four-momentum $p^2 \equiv E^2/c^2 - \vec{p}^2$ exceeds the threshold necessary for the production of two particles, i.e., $p^2 \geqslant (2m)^2 c^2$ with m the particle rest mass and c the speed of light in vacuum. Single particle (and bound) states and continuous multiparticle states lead to the aforementioned respective single poles and branch cuts along the real p^2 axis. We may consider an application of our ideas in the vicinity of zero energy bound states [as in, e.g., the Feshbach resonance of the Bardeen-Cooper-Schrieffer to Bose-Einstein condensate (BCS to BEC) crossover [70–73] in dilute gases where the crossover is driven by varying an attractive contact interaction of strength g] when poles on the real axis are just about to splinter into poles with a infinitesimal imaginary part. Generally, when, by virtue of self-energy corrections, the poles attain a finite imaginary part in the p^2 plane, the corresponding states attain a finite lifetime [with the lifetime being the analog of the correlation length (time) in the two-point correlation functions that we discussed hitherto]. The relations (and exponents) that we derived thus far may be applied, *mutatis mutandis*, for the description of processes associated with the depinning of the poles off the real axis due to the imaginary part of the self-energy Σ, leading to resonances with a finite lifetime. This relates to the scaling of the lifetime τ of resonances in cold atomic gases as a function of $(g_0 - g)$ where g_0 is the strength of the contact interaction at the BCS to BEC crossover point.

IX. CHAOS AND GLASSINESS

Thus far, we have considered phases in which the modulation length is well defined. For completeness, in this section, we mention situations in which aperiodic phases may be observed. The general possibility of such phenomena in diverse arenas is well known [62,74]. We focus here on translationally invariant systems of the form of Eqs. (3) and (4) with competing interactions on different scales that lead to kernels such as

$$v(\vec{k}) = k^4 - c_1 k^2 + c_2, \tag{54}$$

where c_1 and c_2 are positive constants that may give rise to glassy structures for nonzero u. Such a dispersion may arise in the continuum (or small k) limit of hypercubic lattice systems with next-nearest-neighbor interactions (giving rise to the k^4 term) and nearest-neighbor interactions (giving rise to the k^2 term). Within replica type approximations, such kernels that have a finite k minimum (i.e., ones with $c_1 > 0$) may lead to extensive configurational entropy that might enable extremely slow dynamics [42,75].

The simple key idea regarding "spatial chaos" is as follows. It is well known that nonlinear dynamical systems may have solutions that exhibit chaos. This has been extensively applied in the time domain yet, formally, the differential equations governing the system may determine not how the system evolves as a function of the time t, but rather how fields change as a spatial coordinate (x) [replacing the time (t)]. Under such a simple swap of $t \leftrightarrow x$, we may observe spatial chaos as a function of the spatial coordinate x. In general, of course, more than one coordinate may be involved. The resultant spatial configurations may naturally correspond to amorphous systems and realize models of structural glasses. A related correspondence in disordered systems has been found in random Potts systems wherein spin glass transitions coincide with transitions from regular to chaotic phases in derived dynamical analogs [76].

In the translationally invariant systems that form the focus of our study, an effective free energy of the form

$$\mathcal{F}[s] = \frac{1}{2}\int \frac{d^d k}{(2\pi)^d}[v(\vec{k}) + \mu]|s(\vec{k})|^2 + \frac{u}{4}\int d^d x[S^2(\vec{x}) - 1]^2 \tag{55}$$

is generally associated with single component ($n = 1$) systems of the form of Eqs. (4). In Eq. (55), μ represents the deviation from the transition temperature in Ginzburg-Landau theories [or equivalently related to Eq. (45)]. When the constant u in the second term tends to infinity, spin normalization is enforced at all spatial points x. Finite small u corresponds to the so-called "soft-spin" model.

Euler-Lagrange equations for the spins $S(\vec{x})$ are obtained by extremizing the free energy of Eq. (55). These equations are, generally, nonlinear differential equations (as discussed in Appendix B). As is well appreciated, however, nonlinear dynamical systems may exhibit chaotic behavior. In general, a dynamical system may, in the long time limit, either veer towards a fixed point, a limit cycle, or exhibit chaotic behavior. We should therefore expect to see such behavior in the spatial variables in systems which are governed by Euler-Lagrange equations with forms similar to nonlinear dynamical systems. Upon formally replacing the temporal coordinate by a spatial coordinate, chaotic dynamics in the temporal regime map onto to a spatial amorphous (glassy) structure.

In Fig. 8(a), we illustrate the spatial amorphous glasslike chaotic behavior that a one-dimensional rendition of the system of Eq. (54) exhibits. In Figs. 8(b)–8(g), we provide plots of the spatial derivatives of different order versus each other [and $S(x)$ itself].

Another example comes from the spatial analog of dynamical systems with nonlinear "jerks." It is well known that systems with nonlinear "jerks" often give rise to chaos [77]. "Jerk" here refers to the time derivative of a force, or, something which results in a change in the acceleration of a body. Translating this idea from the temporal regime to the spatial regime, one can expect to obtain a aperiodic or glassy structure in a system for which the Euler Lagrange equation (B1) may seem simple. For example, if we have the following Euler Lagrange equation for a particular one-dimensional

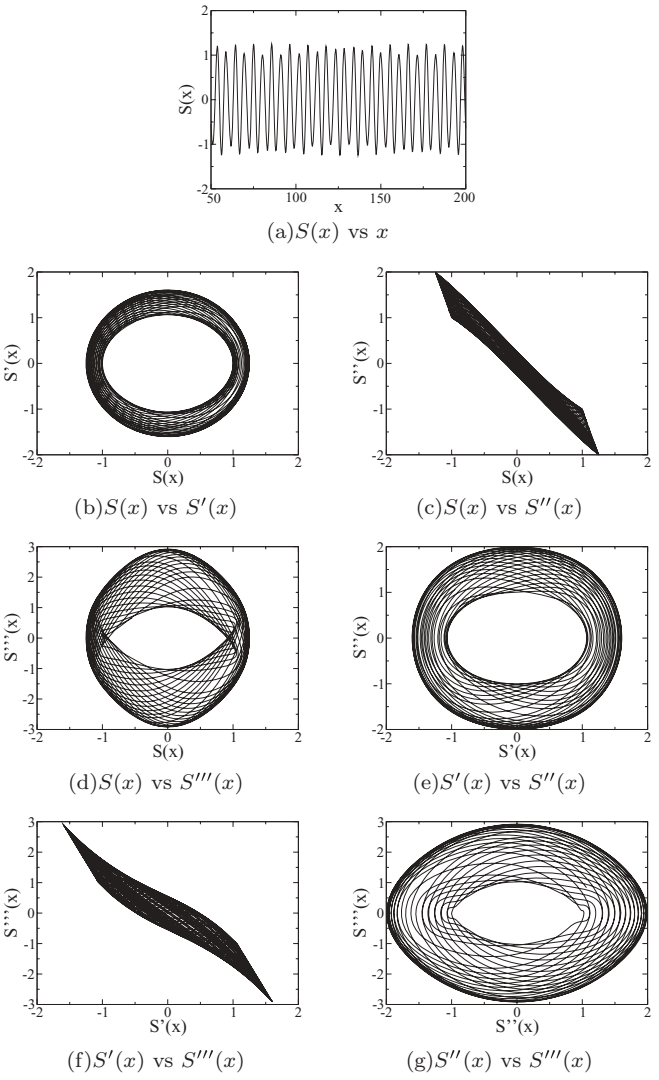

(a) $S(x)$ vs x (b) $S(x)$ vs $S'(x)$ (c) $S(x)$ vs $S''(x)$ (d) $S(x)$ vs $S'''(x)$ (e) $S'(x)$ vs $S''(x)$ (f) $S'(x)$ vs $S'''(x)$ (g) $S''(x)$ vs $S'''(x)$

FIG. 8. Glassiness in system with $v(\vec{k})$ as in Eq. (54) with $c_1 = 5$, $c_2 = 4$ and $u = 1$ and $\mu = 1$ in Eq. (55).

system,

$$S'''(x) = J[S(x), S'(x), S''(x)], \tag{56}$$

with a nonlinear function $J[S(x), S'(x), S''(x)]$, then the system may have aperiodic structure. An example is depicted in Fig. 9.

We now discuss $O(n)$ systems and illustrate the existence of periodic solutions (and absence of chaos) in a broad class of systems. The Euler-Lagrange equations for the system in Eq. (55) [written longhand in Eqs. (B1) and (B7)] become linear in case of "hard" spins, i.e., when the $O(n)$ condition is strictly enforced, i.e., $u \to \infty$. In this limit, all configurations in the system can be described by a finite set of modulation wave vectors (as was the case for the ground states in Sec. V A).

There are several ways to discern this result. First, it may be simply argued that since the Euler-Lagrange equations represent a *finite* set of coupled *linear* ordinary differential equations, chaotic solutions are not present. The configurations, therefore, must be characterized by a finite number of modulation wave vectors.

A second approach is more quantitative. The idea used here is the same as the one used in Ref. [49]. An identical construct

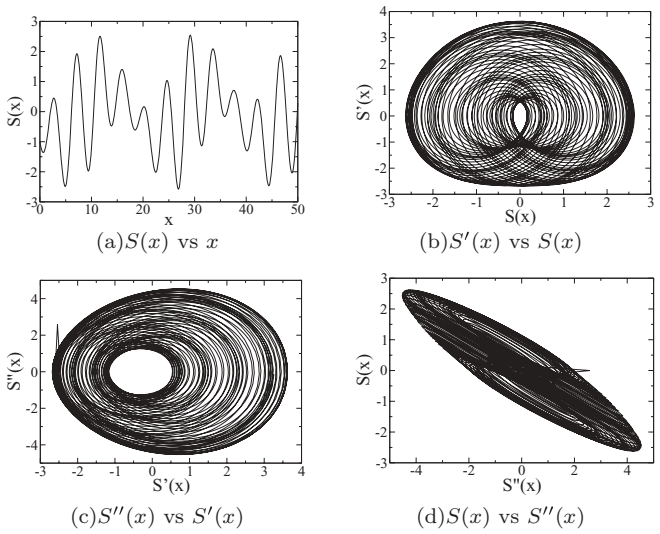

(a) $S(x)$ vs x (b) $S'(x)$ vs $S(x)$

(c) $S''(x)$ vs $S'(x)$ (d) $S(x)$ vs $S''(x)$

FIG. 9. Example of aperiodic structure inspired by system with nonlinear jerks. Here, $J[S(x),S'(x),S''(x)] = -2S'(x) + (|S(x)| - 1)$ and initial conditions are $S(0) = -1$, $S'(0) = -1$, $S''(0) = 1$ (chosen from Ref. [77]).

can be applied to illustrate that spiral and polyspiral states are the only possible states that satisfy the Euler-Lagrange equation if $n > 1$. With v being a functional of the lattice Laplacian of Eq. (7), the lattice rendition of the Euler-Lagrange equations in Fourier space reads as

$$D(\Delta_{\vec{k}})s(\vec{k}) = 0. \tag{57}$$

In what follows, we consider what transpires when the Euler-Lagrange equations have real wave vectors $\mathcal{K} = \{\vec{q}_m\}$ as solutions

$$D(\Delta_{\vec{k}})s(\vec{k})|_{\vec{k}=\vec{q}_m} = 0. \tag{58}$$

To obtain a bound on the number of wave vectors that can be used to describe a general configuration satisfying the Euler-Lagrange equations, we consider general situations wherein (i) $2(\vec{q}_m \pm \vec{q}_{m'}) \neq \vec{k}_{\rm rec}$ for any $\vec{q}_m,\vec{q}_{m'} \in \mathcal{K}$, where $\vec{k}_{\rm rec}$ represents a reciprocal lattice vector; and (ii) $\vec{q}_m \pm \vec{q}_{m'} \neq \vec{q}_p \pm \vec{q}_{p'}$ for any $\vec{q}_m,\vec{q}_{m'},\vec{q}_p,\vec{q}_{p'} \in \mathcal{K}$. Let a particular state be described as

$$\vec{S}_0(\vec{x}) = \sum_m \vec{a}_m e^{-i\vec{q}_m\cdot\vec{x}}, \tag{59}$$

where the vectors $\vec{a}_m$ have n components for $O(n)$ systems. As the states must have real components, the above equation must take the form

$$\vec{S}_0(\vec{x}) = \sum_{m=1}^{N_q} (\vec{a}_m e^{-i\vec{q}_m\cdot\vec{x}} + \vec{a}_m^* e^{i\vec{q}_m\cdot\vec{x}}). \tag{60}$$

In the above, $\vec{a}_m^*$ denotes the vector whose components are complex conjugate those of the vector $\vec{a}_m$. In Eq. (60), we do not count terms involving the wave vectors $\vec{q}_m$ and $-\vec{q}_m$ separately as such terms have been explicitly written in the sum.

We next define the complex vectors $\{\vec{U}_m\}$ and $\{\vec{V}_m\}$ as

$$\vec{U}_m = \vec{a}_m e^{-i\vec{q}_m\cdot\vec{x}}, \quad \vec{V}_m = \vec{a}_m e^{i\vec{q}_m\cdot\vec{x}}. \tag{61}$$

The $O(n)$ normalization condition can then be expressed as

$$\sum_m |\vec{U}_m|^2 = n, \quad \sum_m |\vec{V}_m|^2 = n,$$
$$\sum_{\vec{q}_m - \vec{q}_{m'} = \vec{A}} (\vec{U}_m^* \cdot \vec{U}_{m'} + \vec{V}_{m'}^* \cdot \vec{V}_m)$$
$$+ \sum_{\vec{q}_m + \vec{q}_{m'} = \vec{A}} (\vec{U}_m^* \cdot \vec{V}_{m'} + \vec{U}_{m'}^* \cdot \vec{V}_m) = 0. \tag{62}$$

Solutions to Eq. (62) are spanned by the set of mutually orthonormal basis vectors $\{\vec{U}_m\} \cup \{\vec{V}_m\}$. As these $2N_q$ basis vectors are described by n components each, it follows that

$$N_q \leqslant n/2. \tag{63}$$

Therefore, such states satisfying the Euler-Lagrange equations for an $O(n \geqslant 2)$ system can at most be characterized by $n/2$ pairs of wave vectors. These states can be described by N_q spirals (or "polyspirals"), each of which is described in a different orthogonal plane.

A few remarks are in order.

(i) When u in Eq. (55) is finite, i.e., in the soft-spin regime, polyspiral solutions could be present even though aperiodic solutions are also allowed.

(ii) *Continuum limit*. In the hard-spin limit, i.e., $u \to \infty$ in Eq. (55), if the Fourier space Euler-Lagrange equation is satisfied by nonzero real wave vectors, we have polyspiral solutions as in the lattice case. When u is finite, aperiodic solutions may also be present.

(iii) If the Fourier space Euler-Lagrange equation does not have any real wave-vector solution, polyspiral states are not observed.

In nonlinear dynamical systems, chaos is often observed via *intermittent phases*. As a tuning parameter λ is varied, the system enters a phase in which it jumps between periodic and aperiodic phases until the length of the aperiodic phase diverges. This divergence is characterized by an exponent $\nu = 1/2$ similar to ours [78].

X. CONCLUSIONS

Most of the work concerning properties of the correlation functions in diverse arenas has to date focused on the correlation lengths and their behavior. In this work, we examined the oscillatory character of the correlation functions when they appear.

We furthermore discussed when viable nonoscillatory spatially chaotic patterns may (or may not appear); in these, neither uniform nor oscillatory behavior is found. Our results are universal and may have many realizations. In the following, we provide a brief synopsis of our central results.

(1) We have shown the existence of a universal modulation length exponent $\nu_L = 1/2$ [Eq. (17)]. Here, the scaling could be as a function of some general parameter λ such as temperature. This is observed in systems with analytic crossovers including the commensurate-incommensurate crossover in the ANNNI model.

(2) In certain situations, the above exponent could take other rational values [Eq. (15)].

(3) This result also applies to situations where a correlation length may lock in to a constant value as the parameter λ is varied across a threshold value [as in Eq. (24)].

(4) We extended our result to include situations in which the crossover might take place at a branch point. In this case, irrational exponents could also be present. In Eqs. (37) and (38), we provide universal scaling relations for correlation and modulation lengths.

(5) We illustrate that discontinuous jumps in the modulation and correlation lengths mandate a thermodynamic phase transition.

(6) We showed that in translationally invariant systems (with rotational and/or reflection symmetry), the total number of correlation and modulation lengths is generally conserved as the general parameter λ is varied.

(7) Our results apply to both length scales as well as time scales. We further introduce the notion of a Josephson time scale.

(8) We comment on the presence of aperiodic modulations or amorphous states in systems governed by nonlinear Euler-Lagrange equations. We illustrate that in a broad class of multicomponent systems, chaotic phases do not arise. Spiral or polyspiral solutions appear instead.

(9) Our results have numerous applications. We discussed several nontrivial consequences for classical system in the text. For completeness, in Appendix A, we discuss rather simple applications of our results to noninteracting Fermi systems. We mention situations in which the Fermi surface changes topology, situations with divergent effective masses, and the metal-insulator transition. We further discuss applications to many other systems including Dirac systems and topological insulators. Aside from uniform and regular modulated periodic states of various strongly correlated electronic systems [2–10], there are numerous suggestions and indications of glassy (and spatially nonuniform or chaotic) behavior that naturally lead to high entropy in these systems, e.g., see Refs. [75,79–82]. When spatial modulations are present in the ground states of rotationally invariant (and other) systems, they may lead to "holographiclike" entropy (as in large n renditions) [42]. In future work, we will elaborate on nontrivial consequences of our results for interacting Fermi systems.

Our general analysis regarding the expansion of the inverse correlator G^{-1} as a function of k about points k_* and the myriad conclusions that we draw from it (including exponents) may, in some cases, be viewed as a formal analog of Ginzburg-Landau method of expanding an effective free energy $\mathcal{F}$ in an order parameter field ϕ (i.e., $\delta k \leftrightarrow \phi$ and $G^{-1} \leftrightarrow \mathcal{F}$).

Finally, we make a brief parenthetic remark concerning the "fractal dimension" in glasses and other systems. The notion of fractal dimensionality was recently applied in Ref. [83] based on a comparison between the atomic volume and the reciprocal of the dominant peak K_R in the structure factor in metallic glasses. Specifically, the volume $V \sim K_R^{-D_f}$ with D_f being the fractal dimension. This definition is very intuitive and such a relation between volume and structure factor peaks is to be expected for a system of dimension D_f if all natural scales in the parameter expand or contract with temperature (or other parameters) in unison. However, as we elaborated on at length, aside from global changes in the lattice constant, K_R can change nontrivially with temperature and other parameters in some regular lattice and other systems. Formally, this may give rise to an effective nontrivial fractal dimension in various systems.

ACKNOWLEDGMENTS

The work at Washington University in St. Louis has been supported by the National Science Foundation under NSF Grants No. DMR-1106293 (Z.N.) and DMR-0907793 (A.S.) and by the Center for Materials Innovation. Z.N. thanks the hospitality of the Los Alamos National Laboratory and the KITP during the initial parts of this work. Z.N.'s research at the KITP was supported, in part, by the NSF under Grant No. NSF PHY11-25915. V.D. was supported by the NSF through Grant No. DMR-1005751.

APPENDIX A: FERMI SYSTEMS

In this appendix, we discuss several examples of noninteracting fermionic systems where we observe a correlation or modulation length exponent. We will, in what follows, ignore spin degrees of freedom which lead to simple degeneracy factors for the systems that we analyze. In noninteracting Fermi systems, the mode occupancies are given by the Fermi function. That is,

$$\langle n(\vec{k})\rangle = \langle c^\dagger(\vec{k})c(\vec{k})\rangle = \frac{1}{e^{\beta[\epsilon(\vec{k})-\mu]}+1}, \tag{A1}$$

where we suppressed the spin indices and where $c(\vec{k})$ and $c^\dagger(\vec{k})$ are the annihilation and creation operators at momentum $\vec{k}$ and $\beta = 1/(k_B T)$ with T the temperature. The correlation function associated with the amplitude for hopping from the origin to lattice site $\vec{x}$ is given by

$$G(\vec{x}) = \langle C^\dagger(0)C(\vec{x})\rangle = \sum_{\vec{k}} \langle n(\vec{k})\rangle e^{-i\vec{k}\cdot\vec{x}}, \tag{A2}$$

where $C(\vec{x})$ [and $C^\dagger(\vec{x})$] are the annihilation [and creation] operators for a fermion at site $\vec{x}$.

Thus far, in most explicit examples that we considered, we discussed scaling with respect to a crossover temperature. In what follows, we will, on several occasions, further consider the scaling of correlation and modulation lengths with the chemical potential μ. We will use the letter υ to represent exponents corresponding to scaling with respect to μ and continue to use ν to represent scaling with respect to the temperature T.

The existence of modulated electronic phases is well known [2–13,22,23,84,85]. In particular, the Fermi wave vector dominated response of diverse modulated systems as evident in Lindhard functions, particular features of charge and spin density waves dominated by Fermi surface considerations in quasi-one-dimensional and other systems have long been discussed and have numerous experimental realizations in diverse compounds [84,85]. The exponents that we derived in this work appear for all electronic and other systems in which a crossover occurs in the form of the modulations seen in charge, spin, or other degrees of freedom. Our derived results concerning scaling apply to general interacting systems. To highlight essential physics as it pertains to the change of modulations in systems of practical importance, we briefly review and further discuss free electron systems.

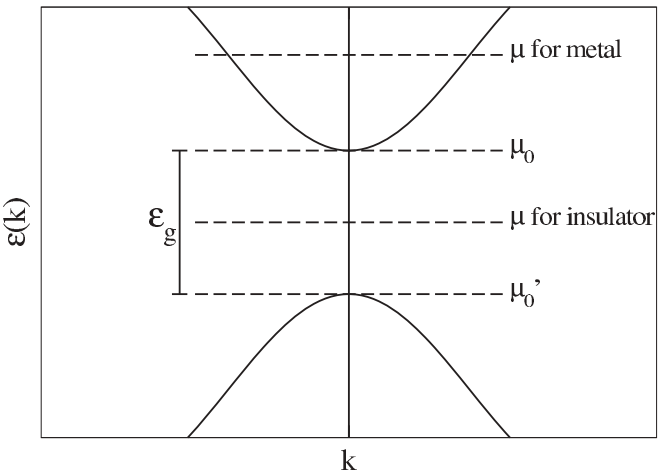

FIG. 10. Transition from a metal to a band insulator. This figure is for illustration only.

1. Zero temperature length scales: Scaling as a function of the chemical potential μ

We first consider a noninteracting fermionic system with a dispersion $\epsilon(\vec{k})$. At zero temperature, the number of particles occupying the Fourier mode $\vec{k}$ is given by

$$\langle n(\vec{k})\rangle = \begin{cases} 1 & \text{for } \epsilon(\vec{k}) < \mu, \\ 0 & \text{for } \epsilon(\vec{k}) > \mu. \end{cases} \tag{A3}$$

All correlation functions, as all other zero temperature thermodynamic properties, are determined by the Fermi surface geometry. We now consider the correlation function of Eq. (A2). This correlation function will generally exhibit both correlation and modulation lengths. To obtain the modulation lengths along a chosen direction (the direction of the displacement $\vec{x}$), a ray along that direction may be drawn. The intercept of this ray with the Fermi surface provides the pertinent modulation wave vectors. As we vary μ, we alter the density ρ via

$$\rho = g_s \int_{\epsilon(\vec{k})<\mu} \frac{d^d k}{(2\pi)^d}, \tag{A4}$$

g_s being the spin degeneracy ($g_s = 2$ for noninteracting spin-half particles such as electrons). As the *Fermi surface topology* is varied, the following effects may be observed.

(1) If two branches of the Fermi surface touch each other at $\mu = \mu_0$ and are disjoint for all other values of μ, then a smooth crossover will appear from one set of modulation lengths to another with $|L_D - L_{D0}| \propto |\mu - \mu_0|$ on both sides of the crossover. This crossover will be associated with an exponent $\upsilon_L = 1$ characterizing the scaling of the modulation lengths with deviations in the chemical potential. An example where a crossover of this kind is realized is the $\epsilon_g = 0$ case of the schematic shown in Fig. 10 in which the crossover occurs at $\mu = \mu_0$. Other examples of this occur at half-filling of the square lattice tight binding model and at three-quarters filling of the triangular lattice tight binding model. These will be discussed later.

(2) If, on the other hand, one branch of the Fermi surface vanishes as we go past $\mu = \mu_0$, the crossover is not so smooth and we get some rational fraction υ_L (usually $\upsilon_L = 1/2$) as the crossover exponent: $|L_D - L_{D0}| \propto |\mu - \mu_0|^{\upsilon_L}$, on one side of the crossover. An example of this is shown in Fig. 11. Here,

$$|L_D - L_{D0}| = \frac{L_{D0}^2}{2\pi}\sqrt{\frac{2|\mu-\mu_0|}{|\epsilon''(2\pi/L_{D0})|}}, \tag{A5}$$

where L_{D0} is the modulation length at the point where the $\mu = \mu_0$ line touches the $\epsilon(k)$ curve, such that $\epsilon'(2\pi/L_{D0}) = 0$. The hopping correlation function takes the form

$$G(x) = \frac{(ax)^{d/2}\mathrm{J}_{d/2}(ax)}{(2\pi)^{d/2}x^d} - \frac{(bx)^{d/2}\mathrm{J}_{d/2}(bx)}{(2\pi)^{d/2}x^d} + \frac{(cx)^{d/2}\mathrm{J}_{d/2}(cx)}{(2\pi)^{d/2}x^d}, \tag{A6}$$

where $\mu_0' < \mu < \mu_0$ and a, b, and c in Eq. (A6) (corresponding to modulation lengths of $2\pi/a$, $2\pi/b$, and $2\pi/c$) are the values of k for which $\epsilon(k) = \mu$ (as shown in Fig. 11).

At arbitrarily small but finite temperatures, the correlation function exhibits modulations of all possible wavelengths. The prefactor multiplying a term with spatial modulations at wave vector $\vec{k}$ is the exponential of $(-|\epsilon(\vec{k}) - \mu|)$. An illustrative example is provided in Fig. 12. Apart from the dominant zero temperature modulations, associated with the wave vector k_2 in Fig. 12, at finite temperature, there are additional contributions

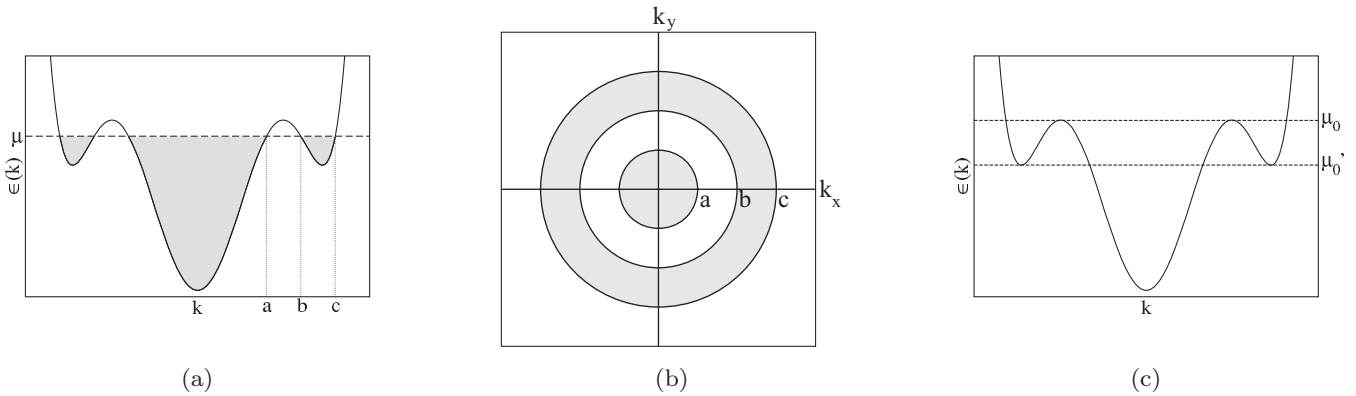

FIG. 11. Example of a Fermi system where the modulation length exponent is 1/2. The gray region shows the filled states. When $\mu > \mu_0$, modulations corresponding to wave vectors $k = a$ and b cease to exist and we get an exponent of 1/2 at this crossover. Similarly, when $\mu < \mu_0'$, modulations corresponding to wave vectors $k = b$ and c die down.

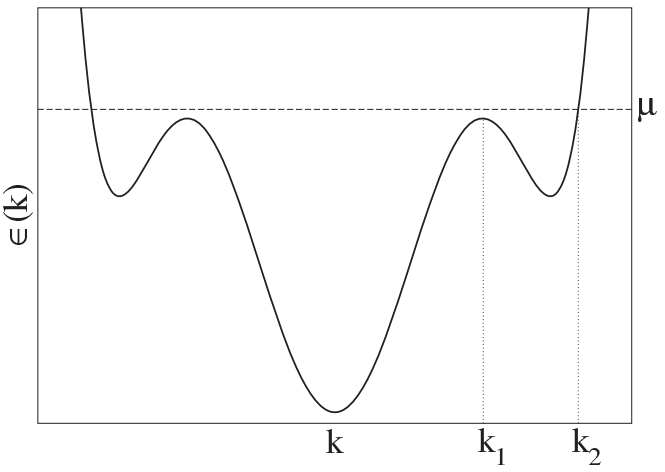

FIG. 12. The same Fermi system as in Fig. 11, but now with a chemical potential $\mu = \mu_0 + \Delta$, slightly higher than μ_0. The temperature is small but finite.

from wave vectors for which $|\epsilon(k) - \mu|$ is small relative to $k_B T$. Near k_2, we can assume $\epsilon(k)$ is linear such that $\epsilon(k) \approx \mu + (k - k_2)\epsilon'(k_2)$. Similarly, near k_1, $\epsilon(k) - \mu \approx -\Delta - (k - k_1)^2\epsilon''(k_1)/2$, where $\Delta = \mu - \mu_0$ (see Fig. 12). For large β, both these contributions are highly localized around k_2 and k_1, respectively, making the above approximations very good and the Fourier transforming integrals easy to evaluate ($\langle n(\vec{k})\rangle$ taking exponential and Gaussian forms). We have

$$G(x) = \frac{(k_2 x)^{d/2} \mathrm{J}_{d/2}(k_2 x)}{(2\pi)^{d/2} x^d} - \frac{2(k_2 x)^{d/2} \mathrm{J}_{d/2-1}(k_2 x)}{(2\pi)^{d/2} \beta \epsilon'(k_2) x^{d-1}} + \frac{e^{-\beta\Delta}(k_1 x)^{d/2} \mathrm{J}_{d/2-1}(k_1 x)}{(2\pi)^{\frac{d-1}{2}} \sqrt{\beta \epsilon''(k_1)} x^{d-1}}, \tag{A7}$$

where $\beta \to \infty$ and $\Delta \to 0$, such that $\beta\Delta \to \infty$.

Next, we will discuss scaling of the modulation length in with the chemical potential, μ in the familiar tight binding models on the square and triangular lattices at zero temperature.

a. Tight binding model on the square lattice

We consider a two-dimensional tight binding model of the square lattice. The dispersion in this model is given by

$$\epsilon(\vec{k}) = -2t(\cos k_x + \cos k_y). \tag{A8}$$

The constant energy contours corresponding to Eq. (A8) are drawn in Fig. 13.

As is clear from Fig. 13, there are certain directions (e.g., along the X axis) along which there is no $\vec{k}$ for $\epsilon(\vec{k}) > 0$. If we consider the same system at zero temperature, the following three crossovers are observed.

(i) *Half-filling*. The chemical potential μ is zero at the half-filling state. The Fermi surface is given by $\pm k_x \pm k_y = \pi$. For small μ, we have

$$\pm k_x \pm k_y = \pi + \frac{\mu}{2t \sin k_x}, \tag{A9}$$

thus giving us an uninteresting modulation exponent, $\upsilon_L = 1$.

(ii) *Empty band*. When $\mu = -4t$, none of the states are occupied. As we increase μ by a tiny amount $\delta\mu$ above this value, we observe a nonzero modulation wave vector $k = \sqrt{\delta\mu/t}$, thus showing a modulation exponent $\upsilon_L = 1/2$.

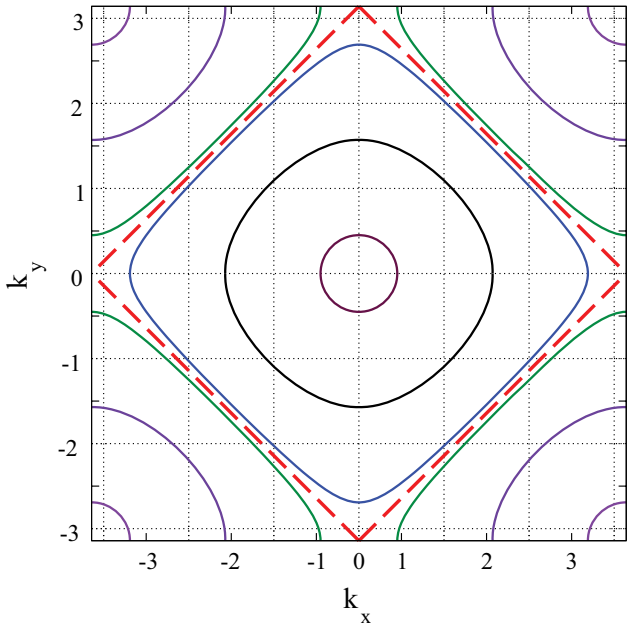

FIG. 13. (Color online) Constant energy contours for two-dimensional tight binding model on the square lattice in Eq. (A8). The red dashed square corresponds to the particle hole symmetric contour where $\epsilon(\vec{k}) = 0$. The contours inside it are for negative $\epsilon(\vec{k})$ and those outside are for positive $\epsilon(\vec{k})$.

(iii) *Full inert bands*. When $\mu = +4t$, all the states are occupied. As we lower μ by a tiny amount $\delta\mu$ below this value, we observe a difference δk of the modulation vector from $\pm\hat{e}_x\pi \pm \hat{e}_y\pi$. We have $\delta k = \sqrt{\delta\mu/t}$, thus showing a modulation exponent $\upsilon_L = 1/2$ again.

b. Tight binding model on the triangular lattice

The analysis of the triangular lattice within the tight binding approximation is very similar to the square lattice discussed above. The dispersion $\epsilon(\vec{k})$ is given by

$$\epsilon(k) = -2t \cos k_x - 4t \cos \frac{k_x}{2} \cos \frac{k_y\sqrt{3}}{2}. \tag{A10}$$

We have exponents similar to the square lattice.

(i) *Three-quarters filling*. The chemical potential $\mu = 2t$ corresponds to the three-quarters filling state. If we concentrate on the $\{k_x = \pi, k_y : -\pi/\sqrt{3} \to \pi/\sqrt{3}\}$ segment (same phenomenon is present at all the other segments of the quarter-filling Fermi surface), we get

$$\delta k_x \sim \frac{\delta\mu}{2\cos\left(\frac{k_y\sqrt{3}}{2}\right)}, \tag{A11}$$

where $k_x = \pi + \delta k_x$ is obtained when $\mu = 2t + \delta\mu$. This leads to a modulation exponent of $\upsilon_L = 1$. The Fermi surfaces for chemical potentials μ close to three-quarters filling are schematically shown in Fig. 14.

(ii) *Empty band*. When $\mu = -6t$, none of the states is occupied. As we increase μ by a tiny amount $\delta\mu$ above

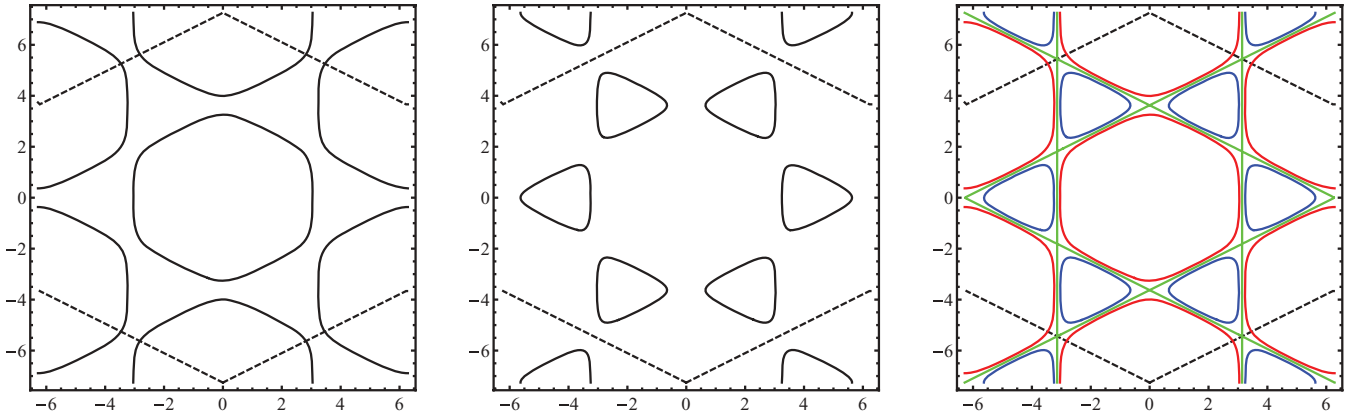

(a) $\mu = 1.8$ (b) $\mu = 2.2$ (c)(Color online) $\mu = 2.2$(blue rounded triangles), $\mu = 2$(green straight lines) and $\mu = 1.8$(red rounded hexagons)

FIG. 14. (Color online) Fermi surface for a triangular lattice with tight binding. The dashed lines are the Brillouin zone boundaries. This demonstrates a smooth crossover from one set of Fermi surface branches to another as μ is changed across $\mu = 2$. The points where the crossovers take place are $(0, \pm 2\pi/\sqrt{3})$, $(\pm\pi, \pm\pi/\sqrt{3})$. The modulation length exponent for this crossover is $\upsilon_L = 1$.

this value, we observe a nonzero modulation wave vector $k = \sqrt{2\delta\mu/3}$, thus showing a modulation exponent $\upsilon_L = 1/2$.

(iii) *Full inert bands*. When $\mu = 3t$, all of the states are occupied, and close to this value the Fermi surface is composed of six small circles around $\vec{k} = \hat{x}\cos(n\pi/3) + \hat{y}\sin(n\pi/3)$, $n = \{0,1,2,3,4,5\}$. If $\mu = 3t - \delta\mu$, we get $|\delta\vec{k}| = 2\sqrt{\delta\mu/3}$, again giving us a modulation length exponent $\upsilon_L = 1/2$.

c. Metal-insulator transition

We discuss here the metal to band insulator transition at zero temperature. In a noninteracting system, this occurs when the Fermi energy is changed such that all occupied bands become completely full, as shown in Fig. 10. In the insulator, the Fermi energy lies in-between two bands and thus the filled states are separated from the empty states by a finite energy gap. As the Fermi energy is tuned, the Fermi energy might touch one of the bands, thereby rendering the system metallic. Close to this transition, the energy is quadratic in the momentum k, i.e., $|k| \propto |\delta\mu|^{1/2}$. This implies that

$$|\delta k| \propto |\delta\mu|^{1/2}. \tag{A12}$$

Following the scaling convention in Eq. (17), we adduce a similar exponent

$$\upsilon_L = 1/2 \tag{A13}$$

that governs the scaling of the modulation lengths with the shift $\delta\mu$ of the chemical potential (instead of temperature variations).

d. Dirac systems

The low energy physics of graphene and Dirac systems is characterized by the existence of Dirac points in momentum space where the density of states vanishes and the energy $\epsilon(k)$ is proportional to the momentum k for small k. When we invoke and repeat our earlier analysis to these systems, we discern a trivial exponent

$$|\delta k| \propto |\delta\mu| \Rightarrow \upsilon_{\text{Dirac}} = 1.$$

This exponent may be contrasted with that derived from Eq. (A13).

e. Topological insulators: Multiple length scale exponents as a function of the chemical potential μ

The quintessential low energy physics of three-dimensional topological insulators can be gleaned from the following effective Hamiltonian [86] in momentum space:

$$H(\vec{k}) = \epsilon_0(\vec{k}) I_{4\times4} + \begin{pmatrix} \mathcal{M}(\vec{k}) & A_1 k_z & 0 & A_2 k_- \\ A_1 k_z & -\mathcal{M}(\vec{k}) & A_2 k_- & 0 \\ 0 & A_2 k_+ & \mathcal{M}(\vec{k}) & -A_1 k_z \\ A_2 k_+ & 0 & -A_1 k_z & -\mathcal{M}(\vec{k}) \end{pmatrix}, \tag{A15}$$

where $\epsilon_0(\vec{k}) = C + D_1 k_z^2 + D_2 k_\perp^2$, $\mathcal{M}(\vec{k}) = M - B_1 k_z^2 - B_2 k_\perp^2$, with $k_\pm = k_x \pm i k_y$, $k_\perp = \sqrt{k_x^2 + k_y^2}$, and A_1, A_2, B_1, B_2, C, D_1, and D_2 constants for a given system. The energy bands are given by

$$\epsilon(\vec{k}) = \epsilon_0(\vec{k}) \pm \sqrt{\mathcal{M}(\vec{k})^2 + A_1 k_z^2 + A_2 k_\perp^2}. \tag{A16}$$

These bands are plotted in Figs. 15(a) and 15(b). The finite gap between the two bands leads to an exponentially damped hopping amplitude, characterized by a finite correlation length when the Fermi energy lies within this gap. These energy bands disperse quadratically for small k, thus yielding

$$|\delta k| \propto \sqrt{|\delta\mu|} \Rightarrow \upsilon_{\text{bulk}} = 1/2 \tag{A17}$$

whenever the correlation length diverges and a insulator to metal transition takes place in the bulk, thus allowing long range hopping. The same exponent is also expected whenever the modulation length becomes constant as μ crosses some threshold value.

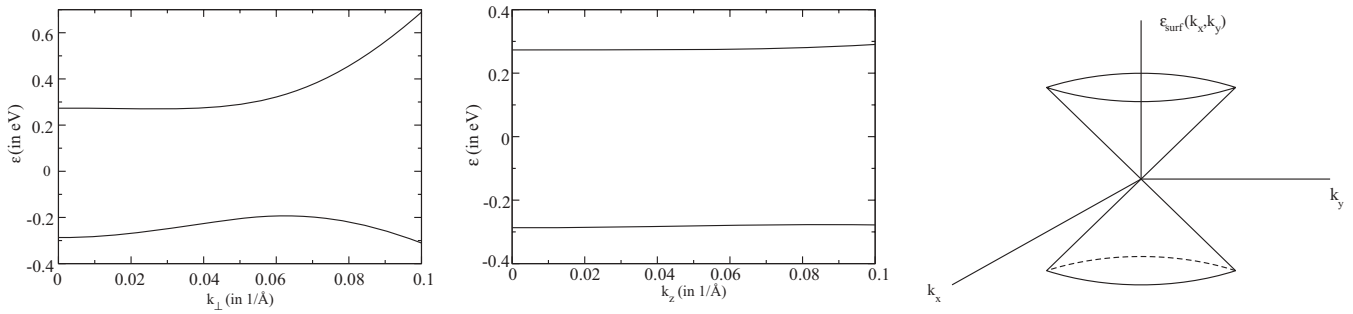

FIG. 15. Energy levels of Bi_2Se_3 topological insulator. (a) $\epsilon(\vec{k})$ as a function of $k_\perp$ at $k_z = 0$; (b) $\epsilon(\vec{k})$ as a function of k_z at $k_\perp = 0$; (c) $\epsilon_{\rm surf}(k_x,k_y)$ as a function of $\vec{k_\perp} \equiv (k_x,k_y)$.

The effective Hamiltonian for the surface states is given by

$$H_{\rm surf} = \begin{pmatrix} 0 & A_2 k_- \\ A_2 k_+ & 0 \end{pmatrix}, \tag{A18}$$

leading trivially to surface energies

$$\epsilon_{\rm surf}(k_x,k_y) = \pm A_2 k_\perp. \tag{A19}$$

Similar to the Dirac points in graphene [see Fig. 15(c)], we trivially find an exponent of

$$\upsilon_{\rm surf} = 1. \tag{A20}$$

f. An example of a zero temperature Fermi system in which υ_L is not half or one

Very large (or divergent) effective electronic masses $m_{\rm eff}$ can be found in heavy fermion systems (and at putative quantum critical points) [87,88]. If the electronic dispersion $\epsilon(\vec{k})$ has a minimum at $\vec{k}_0$, then a Taylor expansion about that minimum is, trivially,

$$\epsilon(\vec{k}) = \epsilon(\vec{k}_0) + \frac{\hbar^2}{2}\sum_{ij}\left(m_{\rm eff}^{-1}\right)_{ij}(k_i - k_{0i})(k_j - k_{0j}) + \sum_{ijl} A_{ijl}(k_i - k_{0i})(k_j - k_{0j})(k_l - k_{0l}) + \dots, \tag{A21}$$

with constants $\{A_{ijl}\}$. When present, parity relative to $\vec{k}_0$ or other considerations may limit this expansion to contain only even terms. As an example, we consider the dispersion

$$\epsilon(k) = c_1 - c_2\left(k^2 - k_0^2\right)^4, \tag{A22}$$

where c_1, c_2 are constants and $c_2 > 0$. The hopping correlation function [of the form Eq. (A2)] of such a system has a term which exhibits modulations at wave vector $k = k_0$ at $\mu = \mu_* = c_1$. At higher values of the chemical potential, such a term ceases to exist. At lower values ($\mu = \mu_* - \delta\mu$), this term breaks up into two terms, the modulation wave vectors of which are different from k_0 by

$$k - k_0 \sim \pm\frac{\delta\mu^{1/4}}{2k_0 c_2^{1/4}} \Rightarrow \upsilon_L = 1/4. \tag{A23}$$

g. Other systems

Numerous realizations in other systems, such as similar quadratic, Dirac type (linear), or other dispersions, were, e.g., found in Hubbard chains [89]. If, in the vicinity of its extrema at $k = q$, the dispersion is generally of the form

$$|\epsilon(k) - \epsilon(q)| \sim |k - q|^z, \tag{A24}$$

then the analysis that we invoked above may be replicated anew. In the general case, we will trivially obtain that

$$\upsilon_L = 1/z. \tag{A25}$$

Equations (A13) and (A14) are particular realizations of this general relation.

2. Finite temperature length scales: Scaling as a function of temperature

At finite temperatures, apart from the modulation lengths, there generally is a set of characteristic correlation lengths. From Eq. (A2), these are obtained by finding the poles (or other singularities) of the Fermi function. Along some direction $\hat{e}_0$, the wave vector $\vec{k}_0 = \hat{e}_0 k_0$ is associated with a pole $k_0 = \pm 2\pi/L_0 \pm i/\xi_0$. At this wave vector,

$$\epsilon(\vec{k}_0) = \mu + \frac{2n+1}{\beta}i, \tag{A26}$$

where n is an integer. For a given μ, let us suppose that as we change the temperature, at $T = T_0$, we reach a saddle point of $\epsilon(\vec{k})$ in the complex plane of one of the Cartesian components of $\vec{k}$. Then, near this saddle point, the corresponding correlation and modulation lengths scale as

$$|L_D - L_{D0}| \propto |T - T_0|^{\nu_L}, \quad |\xi - \xi_0| \propto |T - T_0|^{\nu_c}, \tag{A27}$$

where $\nu_L = \nu_c = 1/2$ in most cases (when the second derivative is not zero).

APPENDIX B: EULER-LAGRANGE EQUATIONS FOR SCALAR SPIN SYSTEMS

We elaborate on the Euler-Lagrange equations associated with the free energy of Eq. (55) in Sec. IX. These assume the

form

$$\int d^d y\, \tilde{V}(\vec{x}-\vec{y})S(\vec{y}) + \mu S(\vec{x}) + u[S^2(\vec{x})-1]S(\vec{x}) = 0, \tag{B1}$$

where $\tilde{V}(\vec{x}) = [V(\vec{x}) + V(-\vec{x})]/2$. For example, if we consider the finite ranged system for which

$$\int d^d y\, \tilde{V}(\vec{x}-\vec{y})S(\vec{y}) = a\nabla^2 S(\vec{x}) + b\nabla^4 S(\vec{x}) + \cdots, \tag{B2}$$

then we will have

$$a\nabla^2 S(\vec{x}) + b\nabla^4 S(\vec{x}) + \cdots + \mu S(\vec{x}) + u[S^2(\vec{x})-1]S(\vec{x}) = 0. \tag{B3}$$

For lattice systems, the Euler Lagrange equation (B1) reads as

$$\sum_{\vec{y}} \tilde{V}(\vec{x}-\vec{y})S(\vec{y}) + \mu S(\vec{x}) + u[S^2(\vec{x})-1]S(\vec{x}) = 0. \tag{B4}$$

In general, it may be convenient to express the linear terms in the above equation in terms of the lattice Laplacian Δ. We write

$$D(\Delta)S(\vec{x}) \equiv \sum_{\vec{y}} \tilde{V}(\vec{x}-\vec{y})S(\vec{y}) + \mu S(\vec{x}), \tag{B5}$$

D being some operator which is a function of the lattice Laplacian Δ. The real space lattice Laplacian Δ, given by the Fourier transform of Eq. (7), acts on a general field f as

$$\Delta f(\vec{x}) \equiv -\sum_{i=1}^{d} [f(\vec{x}+\hat{e}_i) + f(\vec{x}-\hat{e}_i) - 2f(\vec{x})]. \tag{B6}$$

Here, $\{\hat{e}_i\}$ denote unit vectors along the Cartesian directions. (In the continuum limit, Δ can be replaced by $-\nabla^2$.) The Euler-Lagrange equation then takes the form

$$D(\Delta)S(\vec{x}) + u[S^2(\vec{x})-1]S(\vec{x}) = 0. \tag{B7}$$

Equation (B2) corresponds, on the lattice, to

$$\sum_{\vec{y}} \tilde{V}(\vec{x}-\vec{y})S(\vec{y}) = -a\Delta S(\vec{x}) + b\Delta^2 S(\vec{x}) + \cdots. \tag{B8}$$

The Euler Lagrange equation for this finite ranged system reads

$$-a\Delta S(\vec{x}) + b\Delta^2 S(\vec{x}) + \cdots + \mu S(\vec{x}) + u[S^2(\vec{x})-1]S(\vec{x}) = 0. \tag{B9}$$

[1] A. Mesaros, K. Fujita, H. Eisaki, S. Uchida, J. C. Davis, S. Sachdev, J. Zaanen, M. J. Lawler, and E.-A. Kim, Science **333**, 426 (2011).
[2] M. B. Salamon and M. Jaime, Rev. Mod. Phys. **73**, 583 (2001).
[3] B. Kalisky, J. R. Kirtley, J. G. Analytis, J.-H. Chu, A. Vailionis, I. R. Fisher, and K. A. Moler, Phys. Rev. B **81**, 184513 (2010).
[4] J. R. Kirtley, B. Kalisky, L. Luan, and K. A. Moler, Phys. Rev. B **81**, 184514 (2010).
[5] J. M. Tranquada, B. J. Sternlieb, J. D. Axe, Y. Nakamura, and S. Uchida, Nature (London) **375**, 561 (1995).
[6] K. Yamada, C. H. Lee, K. Kurahashi, J. Wada, S. Wakimoto, S. Ueki, H. Kimura, Y. Endoh, S. Hosoya, G. Shirane *et al.*, Phys. Rev. B **57**, 6165 (1998).
[7] S. R. White and D. J. Scalapino, Phys. Rev. Lett. **80**, 1272 (1998).
[8] J. Zaanen and O. Gunnarsson, Phys. Rev. B **40**, 7391 (1989).
[9] Kazushige and Machida, Phys. C (Amsterdam) **158**, 192 (1989).
[10] V. Emery and S. Kivelson, Phys. C (Amsterdam) **209**, 597 (1993).
[11] A. A. Koulakov, M. M. Fogler, and B. I. Shklovskii, Phys. Rev. Lett. **76**, 499 (1996).
[12] M. P. Lilly, K. B. Cooper, J. P. Eisenstein, L. N. Pfeiffer, and K. W. West, Phys. Rev. Lett. **82**, 394 (1999).
[13] R. Du, D. Tsui, H. Stormer, L. Pfeiffer, K. Baldwin, and K. West, Solid State Commun. **109**, 389 (1999).
[14] D. G. Ravenhall, C. J. Pethick, and J. R. Wilson, Phys. Rev. Lett. **50**, 2066 (1983).
[15] G. Watanabe, T. Maruyama, K. Sato, K. Yasuoka, and T. Ebisuzaki, Phys. Rev. Lett. **94**, 031101 (2005).
[16] M. Seul and R. Wolfe, Phys. Rev. A **46**, 7519 (1992).
[17] A. D. Stoycheva and S. J. Singer, Phys. Rev. E **65**, 036706 (2002).
[18] G. Malescio and G. Pellicane, Nat. Mater. **2**, 97 (2003).
[19] G. Malescio and G. Pellicane, Phys. Rev. E **70**, 021202 (2004).
[20] M. A. Glaser, G. M. Grason, R. D. Kamien, A. Kom-rlj, C. D. Santangelo, and P. Ziherl, Europhys. Lett. **78**, 46004 (2007).
[21] C. J. Olson Reichhardt, C. Reichhardt, and A. R. Bishop, Phys. Rev. Lett. **92**, 016801 (2004).
[22] J. Zaanen, Nature (London) **404**, 714 (2000).
[23] S. A. Kivelson, I. P. Bindloss, E. Fradkin, V. Oganesyan, J. M. Tranquada, A. Kapitulnik, and C. Howald, Rev. Mod. Phys. **75**, 1201 (2003).
[24] B. Różycki, T. R. Weikl, and R. Lipowsky, Phys. Rev. Lett. **100**, 098103 (2008).
[25] S. W. Hui and N. B. He, Biochemistry **22**, 1159 (1983).
[26] K. L. Babcock and R. M. Westervelt, Phys. Rev. A **40**, 2022 (1989).
[27] A. Giuliani, J. L. Lebowitz, and E. H. Lieb, Phys. Rev. B **76**, 184426 (2007).
[28] A. Vindigni, N. Saratz, O. Portmann, D. Pescia, and P. Politi, Phys. Rev. B **77**, 092414 (2008).
[29] B. Ma, B. Yao, T. Ye, and M. Lei, J. Appl. Phys. **107**, 073107 (2010).
[30] M. Seul and D. Andelman, Science **267**, 476 (1995).
[31] A. Giuliani, J. L. Lebowitz, and E. H. Lieb, Phys. Rev. B **74**, 064420 (2006).
[32] C. Ortix, J. Lorenzana, and C. Di Castro, Phys. Rev. B **73**, 245117 (2006).
[33] I. Daruka and Z. Gulácsi, Phys. Rev. E **58**, 5403 (1998).
[34] D. G. Barci and D. A. Stariolo, Phys. Rev. B **79**, 075437 (2009).
[35] S. Chakrabarty and Z. Nussinov, Phys. Rev. B **84**, 144402 (2011).
[36] The order of the derivative m in Eq. (12) is zero if $G(k)$ has a pole of finite order at $k = K$, and $m \geqslant 0$ for the branch points.

[37] If we do not have any pole or branch point of the Fourier space correlation function, the form of the real space correlation function is governed by the endpoints of the k-space integration. Therefore, in the continuum, no finite modulation length is allowed. The same is true for the correlation length.

[38] R. J. Elliott, Phys. Rev. **124**, 346 (1961).

[39] M. E. Fisher and W. Selke, Phys. Rev. Lett. **44**, 1502 (1980).

[40] R. B. Griffiths, in *Fundamental problems in statistical mechanics VII: proceedings of the Seventh International Summer School on Fundamental Problems in Statistical Mechanics, Altenburg, F.R. Germany, June 18–30, 1989*, edited by H. van Beijeren (North Holland, 1990), pp. 69–110.

[41] An initial and far more cursory treatment appeared in Z. Nussinov, arXiv:cond-mat/0506554.

[42] Z. Nussinov, Phys. Rev. B **69**, 014208 (2004).

[43] See Eq. (C29) of Ref. [42].

[44] W. Selke, Phys. Rep. **170**, 213 (1988).

[45] Z. Nussinov, J. Rudnick, S. A. Kivelson, and L. N. Chayes, Phys. Rev. Lett. **83**, 472 (1999).

[46] L. Chayes, V. Emery, S. Kivelson, Z. Nussinov, and G. Tarjus, Phys. A (Amsterdam) **225**, 129 (1996).

[47] T. R. Kirkpatrick and D. Thirumalai, J. Phys. A: Math. Gen. **22**, L149 (1989).

[48] G is a function of k^2 for rotationally symmetric systems. Similarly, for a reflection invariant system (invariant under $k_l \to -k_l$), G is a function of (k_l^2) when $k_{l' \neq l}$ are held fixed. The results described in Sec. IV G hold, *mutatis mutandis*, for any component k_l in such reflection invariant systems.

[49] Z. Nussinov, arXiv:cond-mat/0105253; in particular, see footnote [20] therein for the Ising ground states.

[50] S. Chakrabarty and Z. Nussinov, Phys. Rev. B **84**, 064124 (2011).

[51] An $O(n)$ system is one for which the order parameter $\vec{S}(\vec{x})$ has n components normalized as $\vec{S}(\vec{x}) \cdot \vec{S}(\vec{x}) = n$. The large n limit of this system is equivalent to the spherical model where the spins are constrained only by the relation $\sum_{\vec{x}} [S(\vec{x})]^2 = N$, where N is the number of lattice sites. See H. E. Stanley, Phys. Rev. **176**, 2, 718 (1968).

[52] H. E. Stanley, Phys. Rev. **176**, 718 (1968).

[53] T. H. Berlin and M. Kac, Phys. Rev. **86**, 821 (1952).

[54] P. Bak and J. von Boehm, Phys. Rev. B **21**, 5297 (1980).

[55] A. Gendiar and T. Nishino, Phys. Rev. B **71**, 024404 (2005).

[56] S. Redner and H. E. Stanley, J. Phys. C: Solid State Phys. **10**, 4765 (1977).

[57] S. Redner and H. E. Stanley, Phys. Rev. B **16**, 4901 (1977).

[58] J. Oitmaa, J. Phys. A **18**, 365 (1985).

[59] D. Mukamel, J. Phys. A: Math. Gen. **10**, L249 (1977).

[60] R. M. Hornreich, M. Luban, and S. Shtrikman, Phys. Rev. Lett. **35**, 1678 (1975).

[61] K. Zhang and P. Charbonneau, Phys. Rev. B **83**, 214303 (2011).

[62] P. Bak, Rep. Prog. Phys. **45**, 587 (1982).

[63] C. S. O. Yokoi, M. D. Coutinho-Filho, and S. R. Salinas, Phys. Rev. B **24**, 4047 (1981).

[64] C. S. O. Yokoi, M. D. Coutinho-Filho, and S. R. Salinas, Phys. Rev. B **31**, 4502 (1985).

[65] We thank M. Ogilvie for prompting us to think about this generalization.

[66] C. M. Bender and S. Boettcher, Phys. Rev. Lett. **80**, 5243 (1998).

[67] Z. Nussinov, G. Ortiz, and E. Cobanera, Ann. Phys. **327**, 2491 (2012).

[68] B. Josephson, Phys. Lett. **21**, 608 (1966).

[69] M. Peskin and D. Schroeder, *An Introduction to Quantum Field Theory* (Westview Press, Boulder, CO, 2007).

[70] C. A. Regal, M. Greiner, and D. S. Jin, Phys. Rev. Lett. **92**, 040403 (2004).

[71] M. W. Zwierlein, C. A. Stan, C. H. Schunck, S. M. F. Raupach, A. J. Kerman, and W. Ketterle, Phys. Rev. Lett. **92**, 120403 (2004).

[72] T.-L. Ho and R. B. Diener, Phys. Rev. Lett. **94**, 090402 (2005).

[73] Z. Nussinov and S. Nussinov, Phys. Rev. A **74**, 053622 (2006).

[74] H. Thomas, *Nonlinear Dynamics in Solids* (Springer, Berlin, 1992).

[75] J. Schmalian and P. G. Wolynes, Phys. Rev. Lett. **85**, 836 (2000).

[76] D. Hu, P. Ronhovde, and Z. Nussinov, Philos. Mag. **92**, 406 (2012).

[77] J. C. Sprott, Am. J. Phys. **68**, 758 (2000).

[78] Y. Pomeau and P. Manneville, Commun. Math. Phys. **74**, 189 (1980).

[79] T. Park, Z. Nussinov, K. R. A. Hazzard, V. A. Sidorov, A. V. Balatsky, J. L. Sarrao, S.-W. Cheong, M. F. Hundley, J.-S. Lee, Q. X. Jia *et al.*, Phys. Rev. Lett. **94**, 017002 (2005).

[80] S. Pankov and V. Dobrosavljević, Phys. Rev. Lett. **94**, 046402 (2005).

[81] Z. Nussinov, I. Vekhter, and A. V. Balatsky, Phys. Rev. B **79**, 165122 (2009).

[82] J. W. Clark, M. V. Zverev, and V. A. Khodel, arXiv:1203.3201.

[83] D. Ma, A. D. Stoica, and X.-L. Wang, Nat. Mater. **8**, 30 (2009).

[84] G. Grüner, Rev. Mod. Phys. **60**, 1129 (1988).

[85] G. Grüner, *Density Waves In Solids*, Frontiers in Physics (Westview Press, Boulder, CO, 2000).

[86] H. Zhang, C.-X. Liu, X.-L. Qi, X. Dai, Z. Fang, and S.-C. Zhang, Nat. Phys. **5**, 438 (2009).

[87] C. M. Varma, Z. Nussinov, and W. van Saarloos, Phys. Rep. **361**, 267 (2002).

[88] P. Coleman, C. Pépin, Q. Si, and R. Ramazashvili, J. Phys.: Condens. Matter **13**, R723 (2001).

[89] C. Vitoriano and M. D. Coutinho-Filho, Phys. Rev. Lett. **102**, 146404 (2009).